# Phylogenomic insights into the divergent history and hybridization within the East Asian endemic *Abelia* (Caprifoliaceae)

Qing-Hui Sun[1], Diego F. Morales-Briones[2,3], Hong-Xin Wang[1,4], Jacob B. Landis[5,6] Jun Wen[7], Hua-Feng Wang[1]*

[1] *Key Laboratory of Tropical Biological Resources of Ministry of Education, College of Tropical Crops, Hainan University, Haikou 570228, China*

[2] *Department of Plant and Microbial Biology, College of Biological Sciences, University of Minnesota, 140 Gortner Laboratory, 1479 Gortner Avenue, Saint Paul, MN 55108, USA*

[3] *Systematics, Biodiversity and Evolution of Plants, Department of Biology I, Ludwig-Maximilians-Universität München, Menzinger Str. 67, 80638, Munich, Germany*

[4] *Zhai Mingguo Academician Work Station, Sanya University, Sanya 572022, China*

[5] *School of Integrative Plant Science, Section of Plant Biology and the L.H. Bailey Hortorium, Cornell University, Ithaca, NY 14850, USA*

[6] *BTI Computational Biology Center, Boyce Thompson Institute, Ithaca, NY 14853, USA*

[7] *Department of Botany, National Museum of Natural History, MRC-166, Smithsonian Institution, PO Box 37012, Washington, DC 20013-7012, USA*

*Authors for correspondence:

Hua-Feng Wang, E-mail: hfwang@hainanu.edu.cn

## Abstract:

• **Background and Aims** *Abelia* (Caprifoliaceae) is a small genus with six species (including one artificial hybrid). The genus has a disjunct distribution across mainland China, Taiwan, and the Ryukyu islands, providing a model system to explore mechanisms of species dispersal in the East Asian flora. However, the current phylogenetic relationships within *Abelia* remain uncertain.

• **Methods** In this study, we reconstructed phylogenetic relationships within *Abelia* using nuclear loci generated by target enrichment and plastomes from genome skimming. Divergence time estimation, ancestral area reconstruction, and ecological niche modelling (ENM) were used to examine the biogeographic diversification of *Abelia*.

• **Key Results** We found extensive cytonuclear discordance across the genus. Based on nuclear and plastid phylogenies we proposed to merge *A. macrotera* var. *zabelioides* into *A. uniflora.* Network analyses suggested that *A chinensis*, *A. macrotera* and *A. uniflora* are from complex hybrid origins. These hybridization events may explain the complicated taxonomy of the group. Our results show that *Abelia* originated in southwest China, with the nuclear haplotype network suggesting an ancestral haplotype from southwest and central China. The diversification of *Abelia* began in the late Eocene, followed by *A. chinensis* var. *ionandra* colonizing the island of Taiwan in the Middle Miocene. The ENM results suggested an expansion of climatically suitable areas during the Last Glacial Maximum and range contraction during the Last Interglacial. Disjunction between the Himalayan-Hengduan Mountain region (HHM) and the island of Taiwan is most likely the consequence of topographic isolation and postglacial contraction.

• **Conclusions** We used genomic data to reconstruct the phylogeny of *Abelia* and found a clear pattern of reticulate evolution in the group. Overall, our results supported postglacial range contraction together with topographic heterogeneity resulted in the mainland China-Taiwan island disjunction. This study provides important new insights into the speciation process and taxonomy of *Abelia.*

**Key words:** *Abelia*; Gene tree discordance; Hybridization; Mainland China-Taiwan island

disjunction.

## INTRODUCTION

The underlying causes of disjunct distributions in various organisms have been a central issue in biogeography (e.g., Xiang et al., 1998; Wen, 2001; Qian and Ricklefs, 2004; Wang et al., 2012; Wen et al., 2013, 2018). Much discussion has focused on two mechanisms, vicariance and long-distance dispersal (Givnish and Renner, 2004; Yoder and Nowak, 2006; Šarhanová et al., 2017; Wang et al., 2020). The emergence of geographic barriers leads to vicariance, resulting in decreased gene flow; while long-distance dispersal in plants usually involves rare events driven by dispersal vectors such as animals, wind or water currents (Nathan et al., 2008). Recent molecular systematic studies have shown that many plant disjunctions are too young to be explained by continental drift or major geographic barriers (Mummenhoff et al., 2004; Yoder and Nowak, 2006; Linder et al., 2013; Jiang et al., 2019). Hence, long-distance dispersal has emerged as a major mechanism to explain many discontinuous distributions in historical biogeography (Wen et al., 2013; Ye et al., 2019; Wen and Wagner, 2020).

Biogeographic disjunctions between mainland China-Taiwan island have received considerable attention with the separation of the two regions by 130 km (Wu and Wang, 2001; Xiang and Soltis, 2001; Qiu et al., 2011; Chen et al., 2012; Ye et al., 2014, Jin et al., 2020). The island of Taiwan is the largest subtropical mountainous island in the monsoonal western Pacific region, located on the Tropic of Cancer, and originated in the late Miocene (ca. 9-5 million years ago; Sibuet and Hsu, 2004). Molecular phylogenetic analyses have shown that several plant lineages have disjunct distributions between mainland China and Taiwan (e.g., *Sassafras* J. Presl, Nie et al., 2007; *Pseudotsuga* Carrière, Wei et al., 2010; *Triplostegia* Wall. ex DC., Niu et al., 2018; *Prinsepia*., Jin et al., 2020). Geologically, the island of Taiwan and its adjacent continental margin of mainland China belong to the Eurasian plate; in the Late Cretaceous both were part of the continental block. The continental block has undergone many extensions and rifting events since the Paleocene (Wei, 2010; Suo et al., 2015). Two hypotheses have been proposed to explain the formation of current plant disjunctions in this region: long-distance dispersal and postglacial contraction (Chou et al., 2011; Wang et al.,

2013; Ye et al., 2014; Niu et al., 2018). A phylogeographic study of *Cunninghamia* R.Br. ex A.Rich. (Taxodiaceae) revealed that populations of Taiwan derived from continental Asia and colonized the island via long-distance seed dispersal (Lu et al., 2001). Factors that have major impacts on population dynamics and genetic variation patterns in plants in this region include past geological and climatic changes, uplift of the Qinghai-Tibet Plateau, global optimum temperature since the Miocene and the Quaternary glacial-interglacial transition (Xu et al., 2015; Cao et al., 2016; Chen et al., 2020). Recent studies have suggested that although the ice sheet was not ubiquitous from the Qinling Mountains and Huai River (at ca. 34° N) to the tropical south (≤ 22° N) in China during the Last Glacial period, the temperature in most parts of mainland China was lower than today (Shi et al., 2006). Temperature changes influence species distributions, population sizes, and intraspecific genetic differentiation. The postglacial contraction hypothesis states that many species had a continuous distribution from mainland China to Taiwan prior to the Quaternary glacial period, sometimes with disjunctions between the Himalayan-Hengduan Mountain region and the island of Taiwan occurring when samples migrated to higher altitudes as global temperatures increased (Chen and Ying, 2012).

*Abelia* R.Br. belongs to the subfamily Linnaeoideae Raf. within Caprifoliaceae *s.l.* (Dipsacales; Yang and Landrein, 2011; Caprifoliaceae; Wang et al., 2021). The genus includes *A. chinensis* (four varieties), *A. forrestii* (two varieties), *A.* × *grandiflora*, *A. macrotera* (eight varieties), *A. schumannii* and *A. uniflora* (Landrein et al., 2017; 2020; Fig. 1). *Abelia* is a typical East Asian endemic genus with a disjunct distribution in southwestern China, extending to the eastern portion of the island of Taiwan and the Ryukyu islands in Japan. The genus includes an important ornamental species, *Abelia* × *grandiflora*, widely cultivated in yards, parks and roadsides of temperate cities (e.g., Beijing, London, Washington D.C., and Wuhan). However, the phylogenetic relationships within *Abelia* remain unresolved due to limited DNA markers and sampling, and hence the biogeographic history and process of speciation are still uncertain. Kim (1998) used one nuclear (ITS) and one plastid (*matK*) marker to infer the phylogenetic relationships within *Abelia*. However, species relationships could not be clarified because only two *Abelia* species were included, and a

polytomy existed between the two *Abelia* species and those of *Diabelia*. Three *Abelia* species were included (*A. chinensis*, *A. engleriana* and *A. schumannii*) in Jacobs et al. (2010), but no information about relationships can be inferred since the three formed a polytomy. Using ITS and nine plastid regions, Wang et al. (2015) found that *A. forrestii* was sister to all other *Abelia* species, while *A. chinensis* was sister to *A.* × *grandiflora* with moderate support. Although Landrein (2017) included 46 samples (representing five species) of *Abelia* (22 from natural samples and 24 of horticultural breeds), using AFLP, ITS and three plastid genes, the species phylogeny was still unclear due to lack of resolution and low to moderate bootstrap support for many nodes.

Here, we explored the phylogenetic relationships and biogeographic diversification of *Abelia* using a target enrichment dataset for nuclear loci and plastomes from genome skimming. We aim to (1) clarify the species-level phylogeny of *Abelia* based on nuclear genes and plastome data; and (2) reconstruct the biogeographic history of *Abelia* and explore the evolution of its distribution patterns related to the disjunction between mainland China and the island of Taiwan.

## MATERIALS AND METHODS

### *Sampling, genomic data generation*

We sampled 38 individuals from all six species of *Abelia* (Landrein, 2017; 2020). Six Linnaeoideae species [*Diabelia serrata*, *D. sanguinea*, *Kolkwitzia amabilis*, *Dipelta floribunda* (two individuals), *Linnaea borealis*, and *Vesalea occidentails*] were used as outgroups. Voucher specimens were deposited in the herbarium of the Institute of Tropical Agriculture and Forestry of Hainan University (HUTB), Haikou, China. The complete list of samples and information of data sources are provided in Table 1.

DNA was extracted from dried leaf tissue using a modified cetyltrimethylammonium bromide (CTAB) method, with chloroform: isoamyl alcohol separation and isopropanol precipitation at -20□ (Doyle and Doyle, 1987). We checked the concentration of each

extraction with a Qubit 2.0 Fluorometer (Thermo Fisher Scientific, Waltham, MA, USA) and sonicated 400 ng of DNA using a Covaris S2 (Covaris, Woburn, MA) to produce fragments ~150 - 350 bp in length for making sequencing libraries. To ensure that genomic DNA was sheared to the appropriate fragment size, we evaluated all samples on a 1.2% (w/v) agarose gel.

We used a Hyb-Seq approach (Weitemier et al., 2014) combining target enrichment and genome skimming, which allows simultaneous data collection for low-copy nuclear genes and high-copy genomic targets. To obtained nuclear data from target enrichment, we ran MarkerMiner v.1.2 (Chamala et al., 2015) with default settings to identified putative single copy nuclear (SCN) genes, using the transcriptomes of *Lonicera japonica* from 1KP, and the genome of *Arabidopsis thaliana* (L.) Heynh. (Gan et al., 2011) as a reference. Then, we used GoldFinder (Vargas et al., 2019) to further filter the SCN genes identified by MarkerMiner. Finally, we obtained 428 putatively single-copy orthologous genes in total for phylogenetic analysis (Wang et al., 2021). Hybridization, enrichment, and sequencing methods followed those of Wang et al. (2021). We obtained full plastomes from genome skimming data (Wang et al., 2021) with detailed descriptions of plastome sequencing methods in Wang et al. (2020).

### *Read processing and assembly*

Raw sequencing reads were cleaned using Trimmomatic v.0.36 (Bolger et al., 2014) by removing adaptor sequences and low-quality bases (ILLUMINACLIP: TruSeq_ADAPTER: 2:30:10 SLIDINGWINDOW: 4:5 LEADING: 5 TRAILING: 5 MINLEN: 25). Nuclear loci were assembled with HybPiper v.1.3.1 (Johnson et al., 2016). Individual exon assemblies were carried out to avoid chimeric sequences in multi-exon genes produced by potential paralogy (Morales-Briones et al., 2018) and only exons with a reference length of more than 150 bp were assembled. Paralog detection was performed for all exons with the ‘paralog_ investigator’ warning. To obtain ‘monophyletic outgroup’(MO) orthologs (Yang and Smith, 2014), all assembled loci (with and without paralogs detected) were processed following Morales-Briones et al. (2021).

For plastome assembly, raw reads were trimmed using SOAPfilter_v2.2 (BGI, Shenzhen, China). Adapter sequences and low-quality reads with Q-value ≤ 20 were removed. Clean reads were assembled against the plastome of *Kolkwitzia amabilis* (KT966716.1) using MITObim v.1.8 (Hahn et al., 2013). Assembled plastomes were preliminarily annotated with Geneious R11.04 (Biomatters Ltd., Auckland, New Zealand) to detect possible inversions/rearrangements, with corrections of start/stop codons based on published *Abelia* plastomes (*A. chinensis*, accession No. MN384463.1; *A. forrestii*, accession No. MN524636.1; *A.* × *grandiflora*, accession No. MN524635.1; *A. macrotera*, accession No. MN524637.1).

## *Phylogenetic analyses*

*Nuclear dataset*. We analyzed the nuclear data set using concatenation and coalescent-based methods. Individual exons were aligned with MAFFT v.7.037b (Katoh and Standley, 2013) and aligned columns with more than 90% missing data were removed using Phyutility (Smith and Dunn, 2008) prior to concatenation. Maximum likelihood (ML) analysis was conducted using IQ-TREE v.1.6.1 (Nguyen et al., 2015) searching for the best partition scheme (Lanfear et al., 2012) followed by ML gene tree inference and 1000 ultrafast bootstrap replicates (Hoang and Chernomor 2018). Additionally, we used Quartet Sampling (QS; Pease et al., 2018) to distinguish strong conflict from weakly supported branches. We carried out QS with 1000 replicates. We used ASTRAL-III v.5.7.1 (Zhang et al., 2018) for species tree estimation, with the input being individual exon trees generated with RAxML using a GTRGAMMA model.

*Plastome dataset*. Contiguous contigs were aligned with MAFFT v.7.407 (Katoh and Standley, 2013) and columns with more than 90% missing data were removed using Phyutility. We performed extended model selection (Kalyaanamoorthy et al., 2017) followed by ML gene tree inference and 200 non-parametric bootstrap replicates for branch support in IQ-TREE. Additionally, we evaluated branch support with QS using 1,000 replicates.

## *Species network analysis*

Due to computational restrictions and given our primary focus on potential reticulation between different species, we reduced the 45-sample data set to one outgroup and 14 ingroup samples representing all major clades based on the nuclear analyses. We looked for evidence of hybridization within *Abelia* via species network search carried out with the InferNetwork_MPL function in PhyloNet (Wen et al., 2018). Network searches were carried out using only nodes in the gene trees that had at least 50 percent bootstrap support, enabling up to five hybridization events and optimizing the branch lengths and probabilities of inheritance of the returned species networks under the full probability. To disentangle nested hybridization, we also created a reduced, 12-sample data set by removing three known hybrids (*A.*× *grandiflora* E159, *A.*× *grandiflora* E227 and *A. chinensis* E206; see results) and carried out analyses as previously described. We used the command 'CalGTProb' in PhyloNet to calculate the probability scores of the concatenated RAxML, ASTRAL, and plastid trees, given individual nuclear gene trees, to estimate the optimal number of hybridizations and to test if the network model explained our gene trees better than a purely bifurcating tree. We selected the best-fit-species network model using the lowest values for bias-corrected Akaike information criterion (AICc; Sugiura, 1978), Akaike information criterion (AIC; Akaike, 1998), and the Bayesian information criterion (BIC; Schwarz, 1978).

## *Genetic diversity and population structure*

Because increasing the quantity of missing data in the 'median' ($Fst \approx 0.15$) and 'maximum' ($Fst > 0.15$) SNP matrices can lead to skewed estimations of *Fst* (Hodel et al., 2017), we only used the 'minimum' data set for genetic diversity analysis. We used BAYESCAN v.2.1 (Foll and Gaggiotti, 2008; Cao et al., 2016) to calculated genetic distance (*Fst*) for nuclear gene loci, to define the 'minimum' dataset ($Fst < 0.15$). All parameters were kept at default settings except for modifying the *a priori* odds of the neutral model to 250 (Foll and Gaggiotti, 2008).

DnaSP v.5 (Librado and Rozas, 2009) was used to analyze nucleotide polymorphisms and haplotypes from population of each species in the 'minimum' data set. NETWORK v.5.0.0.3 (Bandelt et al., 1999) was used to visualize the haplotype network diagrams of each species. We estimated genetic diversity indices including nucleotide diversity ($\pi$), expected heterozygosity (*He*), observed heterozygosity (*Ho*) and inbreeding coefficients (*Fis*) using GenAlEx v.6.1(Peakall and Smouse, 2006).

Bayesian clustering of individuals was conducted using STRUCTURE v. 2.3.4 (Pritchard et al., 2000) for *Abelia* using the 'minimum' data set. Ancestral genetic populations (K) were determined using an admixture model assuming correlated allele frequencies. The length of the burn-in period and the MCMC (Markov Chain Monte Carlo algorithm) runs were set to 50,000 and 500,000, respectively. Three runs for each K value (K = 1-10) were used to estimate the most likely value of K using $\Delta$K (Evanno et al., 2005) after combining with Clumpp v.1.1.2b (Jakobsson and Rosenberg, 2007) and analyzing with Structure Harvester v.0.6.94 (Earl, 2012).

### *Divergence time estimation*

To examine the historical biogeography of *Abelia*, we performed a dated phylogenetic analysis using BEAST v.1.8 (Drummond et al., 2012). As there is potential ancient hybridization in *Abelia*, we estimated dates separately using the nuclear and plastid data. We selected the fruit fossil of *Diplodipelta* from the late Eocene Florissant flora of Colorado (Manchester, 2000; Bell and Donoghue, 2005) to calibrate the node containing *Diabelia* and *Dipelta*, as the fossil shows morphological similarities to the two genera. We set a lognormal prior for the divergence at the stem of *Diabelia* and its sister clade *Dipelta* (offset 36 Ma, log-normal prior distribution 34.07-37.20 Ma). The ancestral node of Linnaeoideae (the root of our tree) was constrained to 50.18 Ma (mean 50.18 Ma) from results of previous studies (Wang et al., 2021) despite the lack of fossil evidence. The BEAST analyses were performed using an uncorrelated log normal (UCLN) relaxed clock with a Yule tree prior, random starting trees, and GTR + G as model of sequence evolution (as selected by MrModelTest

v.2.3; Nylander et al., 2004). Each MCMC run was conducted for 100,000,000 generations with sampling every 5,000 generation. The first 10% of trees were discarded as burn-in. We used Tracer v.1.6 to assess convergence and effective sample size (ESS) > 200 (Rambaut et al., 2014). Tree Annotator v.1.8.0 (Drummond et al., 2012) was used to summarize the set of post-burn-in trees and their parameters in order to produce a maximum clade credibility chronogram showing the mean divergence time estimates with 95% highest posterior density (HPD) intervals. FigTree v.1.4.2 (Drummond et al., 2012) was used to visualize the resulting divergence times.

### *Ancestral area reconstructions*

We reconstructed the historical biogeography of *Abelia* using the Bayesian binary MCMC (BBM) analysis implemented in RASP v.3.21 (Yu et al., 2015). To account for phylogenetic uncertainty, 5,000 out of 20,000 post-burn-in trees from the BEAST analyses (nuclear data) were randomly chosen for the BBM analyses. We compiled distribution data for the species of *Abelia* and assigned the included taxa to their respective ranges. Considering the areas of endemism in *Abelia* and tectonic history of the continent, we used three areas: (A) Southwest China, (B) Central-East China, and (C) Taiwan and Ryukyu islands. Each sample was assigned to its respective area according to its contemporary distribution range (Table 1). We set the root distribution to null, applied 10 MCMC chains each run for 100 million generations, sampling every 10,000 generations using the JC + G model. The MCMC samples were examined in Tracer v.1.6 (Drummond et al., 2012) to confirm sampling adequacy and convergence of the chains to a stationary distribution.

### *Ecological niche modelling*

We performed Ecological Niche Modelling (ENM) on *Abelia* using MAXENT v.3.2.1 (Phillips et al., 2006). For the input we obtained 200 species occurrence data points from the Chinese Virtual Herbarium (CVH, https://www.cvh.ac.cn/), Global Biodiversity Information

Facility (http://www.gbif.org/) and field observations. The details of these occurrence data are listed in Table S1. We used 19 bioclimatic variables as environmental data for ENM representing five different time periods. Past and current data for these variables were available from the WorldClim database (http://worldclim.org/). The data included baseline climate (BioClim layers for the period 1950-2000 at a spatial resolution of 30 s arc), data for the last glacial maximum (LGM; ~22 000 years BP) with spatial resolution at 2.5 min arc resolution simulated by Community Climate System Model (CCSM), Max Planck Institute Model (MPI) and Model for Interdisciplinary Research on Climate (MIROC), and the last interglacial period. Replicate runs (25) of MAXENT were performed to ensure reliable results. Model performance was assessed using the area under the curve (AUC) of the receiver operating characteristic. AUC scores may range between 0.5 (randomness) and 1 (exact match), with those above 0.9 indicating good performance of the model (Swets, 1988). The MAXENT jackknife analysis was used to evaluate the relative importance of the 19 bioclimatic variables employed. All ENM predictions were visualized in ArcGIS v.10.2 (ESRI, Redlands, CA, USA).

### *Data accessibility*

Raw Illumina data from target enrichment is available at the Sequence Read Archive (SRA) under accession SUB7674585 (see Table 1 for individual sample SRA accession numbers). DNA alignments, phylogenetic trees and results from all analyses and datasets can be found in the Dryad data repository.

## RESULTS

### *Exon assembly*

The number of assembled exons per species ranged from 253 (*A. macrotera* var. *macrotera* E45) to 992 (*A. uniflora* E46) (with > 75% of the target length), with an average of 851 exons per sample (Table S2; Fig. S1). The number of exons with paralog warnings

ranged from 6 in *A. macrotera* var. *macrotera* E45 to 698 in *A. uniflora* E46 (Table S2). The concatenated alignment had a length of 365,330 bp, including 22,045 parsimony-informative sites, and a matrix occupancy of 83% (Table 2). The smallest locus had a length of 150 bp, while the largest locus had a length of 3,998 bp. The plastid alignment resulted in a matrix of 163,130 bp with 3,850 parsimony-informative sites and a matrix occupancy of 96% (Table 2).

### *Phylogenetic reconstruction*

We inferred the Abelia phylogeny based on nuclear and plastid alignments (Figs. 2-3 and S2-3). Despite the generally well-supported topology, the positions of clades representing *A.* × *grandiflora*, *A. uniflora* and *A. macrotera* clade were unstable across all analyses. Phylogenetic reconstructions based on nuclear concatenation data showed all of the major clades with relationships well supported (BS ≥ 75%; Fig. 2, Left). *Abelia schumannii* is nested within *A. macrotera*, and sister to *A. macrotera* var. *macrotera* E45, with the QS analysis showing moderate support (0.5/0.92/1, Fig. S2, Left). *Abelia chinensis* forms a clade with *A.* × *grandiflora*; and *A. macrotera* var. *zabelioides* is sister to *A. uniflora* with the clade having strong QS support but also a signal of a possible alternative topology (0.97/0/1, Fig. S2, Left). The *A. chinensis* + *A.* × *grandiflora* clade is then sister to the *A. macrotera* var. *zabelioides* + *A. uniflora* clade (Fig. 2, Left).

The ASTRAL analyses (Fig. 3) recovered all major clades with strong support (local posterior probabilities, LPP ≥ 0.95). Similar to the ML concatenation nuclear tree, *A. schumannii* is nested within *A. macrotera*. The *A. chinensis* + *A.* × *grandiflora* clade is sister to the remaining species. *Abelia forrestii* is sister to *A. macrotera* + *A. schumannii* clade, which is then sister to *A. macrotera* var. *zabelioides* + *A. uniflora*. The clade composed of *A. chinensis* + *A.* × *grandiflora* has moderate QS support with signal for a possible alternative topology (0.33/0.06/0.99). The clade composed of *A. macrotera* var. *zabelioides* + *A. uniflora* has strong QS support but a signal of a possible alternative topology (0.98/0/1). The sister relationship of the *A. macrotera* var. *zabelioides* + *A. uniflora* has QS counter support as a clear signal for alternative topology (-0.21/0.32/0.99).

For the plastid tree (Fig. 2, Right and S3), *Abelia schumannii* was nested within *A. macrotera*, and sister to *A. macrotera* var. *macrotera* E45, with the QS analysis showing moderate support (0.27/0.18/0.91). *Abelia uniflora* is sister to *A. macrotera* var. *zabelioides*, with the clade having strong QS support signaling an alternative topology (0.51/0.35/0.98). The *A. chinensis* + *A.* × *grandiflora* clade shows a sister relationship with the *A. macrotera* var. *zabelioides* + *A. uniflora* + *A. macrotera* + *A. schumannii* clade, with strong QS support (0.75/0.51/0.98). The results strongly support *A. forrestii* from Yunnan as sister to the remainder of the genus with the QS analysis providing full support (1/–/1, Fig. S3).

In our species network analyses (including both 15 and 12 samples), all networks with one to five reticulations events were shown to be a better model than a strictly bifurcating tree (Table 3; Figs. 4 and S4-5). Four reticulation events were inferred for the best networks in the 15-sample tree, the two reticulation-events involving *A.* × *grandiflora*, the third reticulation event revealed *A. chinensis* and the fourth reticulation event revealed ancestral gene flow in the *A.* × *grandiflora* clade (Fig. 4A). For *A.* × *grandiflora* E159, the inheritance probability analysis showed that the major genetic contributor (57.2%) came from the ancestor of *A.* × *grandiflora* and a minor contributor was from the *A. macrotera* clade (42.8%). For *A.* × *grandiflora* E227, the major genetic contributor came from *A. uniflora* (53.6%). For *A. chinensis* E206, the major genetic contributor (53.0%) came from the ancestor of *A.* × *grandiflora*. For the ancestor of the *A.* × *grandiflora* clade, the major genetic contributor was a putative ancestor of *A. chinensis* (74.1%) with a minor contribution from *A. uniflora* (25.9%). In the 12-sample tree (Fig. 4B), we removed the known hybrids from the previous analyses, excluding *A.* × *grandiflora* E159, *A.*× *grandiflora* E227 and *A. chinensis* E206, and then discovered that the best network had three reticulation events. There appears to be abundant gene flow in the backbone of *Abelia* and the 12-sample analyses showed that *A. macrotera*, *A. uniflora* and *A. chinensis* were each derived from complex hybrid origins.

## *Population structure*

We used BAYESCAN v.2.1 to obtain a total of 788 genes ($Fst < 0.15$, Fig. S6). Fifteen

haplotypes (H1-15) were identified across the 12 populations of *Abelia* (Fig. 5). Five haplotypes (H3, H5, H9, H12 and H13) were found to be shared by multiple species. H3 was a shared haplotype between *A. macrotera* var. *engleriana* and *A. chinensis*. H5 was a shared haplotype between *A. uniflora* and *A. macrotera*. H9 was shared by *A. macrotera* var. *mairi*, *A. macrotera* var. *deutziaefoli*a, *A. macrotera* var. *zabelioides* and *A. macrotera* var. *engleriana*. H12 is unique to *Abelia chinensis* var. *ionandra*. H13 was a shared haplotype between *A. chinensis* var. *ionandra* and *A. chinensis*. There were three haplotypes (H3, H8 and H9), mainly distributed in southwestern China (e.g., Chongqing, Guizhou, Sichuan and Yunnan), with the diversity ranging from 0.139 to 0.176 (Fig. 5, Table. S3). There were six haplotypes (H2, H7, H9, H10, H11 and H15) distributed in central China (e.g., Hubei), with the diversity is 0.477. There were six haplotypes (H1, H5, H7, H12, H13 and H14) distributed in eastern China (e.g., Fujian), southern portion of the island of Taiwan, and southern Japan (Fig. 5).

The results of the STRUCTURE analyses based on the BAYESCAN markers are presented in Fig. 5, the values of the log-likelihood of the data, log Pr(K), increased progressively with the increase in K. According to Evanno's approach, K = 4 was the most likely number of genetic clusters for 0.5 million generations. The results of STRUCTURE suggests that there is gene flow among the four species (Fig. 5).

## *Divergence time estimation*

Divergence time estimates based on the nuclear tree (Fig. 6) suggested that the crown group of *Abelia* originated 33.57 Ma (95% HPD: 29.16-37.55 Ma, node 1). The *A. chinensis* clade was dated to have diverged from the remaining *Abelia* species at 31.82 Ma (95% HPD: 27.57-37.10 Ma, node 2). The the split between *A.* × *grandiflora* and all varieties of *A. chinensis* was dated to 25.09 Ma (95% HPD: 19.00-33.80 Ma, node 4). The split between *A. macrotera* var. *deutziaefolia* and *A. macrotera* var. *engleriana* was dated to 18.53 Ma (95% HPD: 16.72-23.31 Ma, node 8). The split between *A. uniflora* and *A. macrotera* var. *zabelioides* was dated to 18.33 Ma (95% HPD: 15.09-22.12 Ma, node 9). The split time

between *A. macrotera* and *A. schumannii* was 6.78 Ma (95% HPD: 4.92-11.29 Ma, node 12). The crown of *A. forrestii* was 4.61 Ma (95% HPD:1.88-6.71 Ma, node 14). Most diversification events within *Abelia* dated to the Early to Middle Miocene (Fig. 6). A comparison of the time estimates using the chloroplast tree is shown in Fig. S7. For instance, the age of the crown group of *Abelia* was dated to 45.10 Ma (95% HPD: 31.82-50.09 Ma, node 1). The split between *A. uniflora* and *A. macrotera* var. *zabelioides* was 35.07 Ma (95% HPD: 25.00-39.88 Ma, node 4). The split between *A. macrotera* and *A. schumannii* was 31.79 Ma (95% HPD: 18.39-38.15 Ma, node 5).

## *Ancestral area reconstruction*

According to our ancestral area reconstructions paired with divergence time estimation, *Abelia* originated around the late Eocene (Fig. 6) in mainland China (Fig. 7). Our analyses revealed four dispersal events and two vicariance events among the three defined biogeographic areas (Fig. 7). The ancestor of *Abelia* was inferred to have been present throughout region A (Yunnan, Chongqing, Sichuan, Guizhou and Hubei) and B (Jiangxi and Fujian), with subsequent dispersal or vicariance across southeast China. The results indicate a southwest China origin for the genus *Abelia*.

## *Ecological niche modelling and niche identity tests*

The AUC test result (mean ± SD) for the ENM, averaged across all 25 runs, was significant (0.996 ±0.000 for *A. chinensis* and 0.993± 0.001 for *A. uniflora*) (Figs. 8 and S8), which supports the predictive power of the model. The MaxEnt analyses show that the current distribution prediction is largely identical to the recorded distribution of *Abelia*, and expansion of distribution beyond the existing range is also reasonable, including *A. uniflora* populations along the narrow coastline of eastern China and Japan (Fig. S8). In our analysis, the LGM climate and the present time climate species distribution areas show different distribution patterns. We used CCSM, MIROC and MPI models to simulate the LGM climate

for five species of *Abelia* with the distribution of the two LGM models (CCSM and MPI models) being highly similar. For the CCSM and MIROC models (the MIROC model area simulation during the LGM period is warmer and drier than the CCSM model), the distribution density and range of *Abelia* under the MPI model was slightly lower than the distribution density and range under the CCSM model, but the differences were not significant (Fig. S8). Compared with the LGM climate, the potential distribution range of *Abelia* species in mainland China will be much smaller, while the habitat remains stable in most of the present time climate distributions.

# DISCUSSION

## *Phylogenetic relationships within Abelia*

This study reconstructed well-supported phylogenetic relationships for *Abelia* using both nuclear and plastid data (Figs. 2-3 and S2-3). The inferred topologies of the four recognized species in the nuclear and plastid trees were different from each other (Figs. 2-3 and S2-3), but also share many commonalities. For instance, *Abelia schumannii* is nested within *A. macrotera*, and *A. macrotera* var. *zabelioides* is sister to the *A. uniflora* clade. In addition, these nodes have strong QS support values. Cytonuclear discordance has been widely detected in plants. The three main reasons for cytonuclear discordance are gene duplication/extinction, horizontal gene transfer/hybridization, and incomplete lineage sorting (ILS), but sources of such discordance remain hard to disentangle, especially when multiple processes co-occur (Degnan and Rosenberg, 2009).

*Abelia macrotera* var. *zabelioides* and *A. uniflora* share a similar origin (Landrein et al., 2017), which indicates that *A. macrotera* × *chinensis* formed from different hybridization events at different times as shown in our species network analyses (Fig. 4). We also found that *A. macrotera* var. *zabelioides* and *A. uniflora* show many similarities in morphology (i.e., single-flowered inflorescence, red corolla, and two sepals). Landrein (2020) reported that the *A. uniflora* group contains *A. macrotera* var. *zabelioide*s.

Our results are consistent with Jacobs et al. (2010) in terms of *A. schumannii* being nested within *A. macrotera*. Additionally, *A. schumannii* has no independent ecological niche, and its distribution overlaps with *A. macrotera* (Landrein et al., 2020). However, this does not necessitate that *A. schumannii* is a synonym of *A. macrotera* since we have only sampled one accession of *A. schumannii*. A single accession is likely not enough since we are not capturing any genetic variation within *A. schumannii*. Therefore we need to expand the sampling of *A. schumannii* in future studies.

## *Hybridization and introgression*

Over many decades, evolutionary studies have focused on hybridization, the crossbreeding of individuals from different species, and introgression, the transfer of genes across species mediated largely by backcrossing (Rieseberg and Carney, 1998; Grant PR and Grant BR, 2019; Rendón-Anaya et al., 2019; Nwankwo et al., 2019). The *A. uniflora* complex is the most enigmatic complex in the genus, though it was only briefly described by Wallich (1829). Members of the *A. uniflora* complex are often difficult to identify using morphological characters alone. The morphological differences among entities within the *A. uniflora* complex can be explained by one or several historical or ongoing evolutionary processes. Specifically, the null taxonomic hypothesis is that the *A. uniflora* complex is a single hyperdiverse species (Link-Pérez, 2010), while the alternative is that speciation has occurred or is occurring. We expect to detect clear genetic differentiation which may be stronger if speciation is complete, or weaker if it is ongoing or confounded by introgression (Nosil, 2008; Liu et al., 2018). Based on morphological evidence and AFLP data, Landrein et al. (2017) indicated that *A. uniflora* shows evidence of formation due to hybridization and introgression between *A. macrotera* and *A. chinensis*. Examples of similar speciation events in different families were cited in Li et al. (2011), and the hypothesis put forward was glaciation survival east and west of the Mekong-Salween divide. Glaciation may have led to the isolated distribution of *A. forrestii.* Repeated hybridization and introgression tend to blur the lines between hybrids and their parents. Landrein et al (2017) showed that *A. forrestii*

occurs in the contact zone between *A. macrotera* and *A. chinensis*, leading to the hypothesis that hybridization and introgression between *A. macrotera* and *A. chinensis* led to the emergence of *A. forrestii*.

We find that *A.* × *grandiflora* is sister to *A. chinensis* in the inferred phylogenies (Figs. 2, 3) and our network analyses further confirm the hybrid origin of *A.* × *grandiflora* from *A. chinesis* and *A. uniflora* (Fig. 4A). Landrein et al. (2017) found that *A. uniflora* formed a clade with *A.* × *grandiflora* and they reported that the hybrid origin of cultivated *A.* × *grandiflora* involving *A. uniflora* as one progenitor, but the other progenitor could not previously be identified. They speculated that the second progenitor was *A. chinensis* or to a lesser extent *A. macrotera* based on their phylogenetic analysis, or even a hybrid individual between the two (*A. chinensis* and *A. macrotera*).

Landrein et al. (2017) highlighted the genetic distinction between *A. uniflora* and *A. macrotera*, two taxa that are often difficult to identify based on morphology alone (Fig. 1). Our results indicate that a clear disjunction in their distribution exists (Fig. 3). West-to-east disjunctions across China have also been described in other genera and species, with some being hypothesized to form from allopatric incipient speciation (Qiu et al., 2009a). In our study, the identity and origin of *A.* × *grandifolia*, a hybrid between *A. chinensis* and *A. uniflora*, is weakly supported, while *A. uniflora* shows evidence of allopatric speciation due to hybridization and introgression between *A. macrotera* and *A. chinensis* (Table 3; Figs. 4, S4-5). In the STRUCTURE analysis, we found clear evidence of hybridization among the four species (Fig. 5), however, the full extent of hybridization is difficult to assess as it is represented by relatively few samples. In addition, a substantial amount of discordance in the main branches of *Abelia* exist, and the network (12-sample) analyses (Fig. 4B) showed that *A. macrotera*, *A. uniflora*, and *A chinensis* all have complex hybrid origins. This is a potential reason why the taxonomy of this group has been historically complicated.

## *Biogeographic diversification history of Abelia*

In this study, divergence time estimates from inferred from nuclear (Fig. 6) and

chloroplast data (Fig. S7) show stark differences. Simulation studies have revealed that methods for inferring species trees are likely to be relatively resistant to intra-locus recombination (Lanier and Knowles, 2012; Wang and Liu, 2016). In our analysis, the molecular clock estimates of the species tree indicate that the crown of *Abelia* dates to the late Eocene 33.57 Ma (95% HPD: 29.16-37.55 Ma) (Fig. 6). Our phylogenetic analyses indicate that *A. chinensis* var. *ionadra* from the island of Taiwan is sister to *A. chinensis* from Jiangxi province, China (Figs. 2-3 and S2-3). In addition, previous phylogenetic and phylogeographic studies have generally shown that existing populations of many species on the island of Taiwan are descendants of mainland China (e.g., *Taiwania*, Chou et al., 2011; *Sassafras*, Nie et al., 2007; *Dichocarpum arisanense*, Xiang et al., 2017; *Triplostegia*, Niu et al., 2018), with no reported cases supporting a reverse direction of dispersal. Based on our time estimates, the stem age of *A. chinensis* var. *ionadra* was dated to the Middle Miocene, ca. 18.59 Ma (Fig. 6, node 8), which greatly predates the formation of the island of Taiwan, which originated in the Late Miocene (Sibuet and Hsu, 2004). A similar disjunction predating the formation of Taiwan is shown in *Tinospora dentata* which split from its Japanese relatives in the Early Oligocene around 38.97 Ma (95% HPD: 26.45-52.52) (Wang et al., 2017).

The island of Taiwan is located at the eastern edge of the Eurasian plate and the Taiwan Strait could have first occurred in the Late Mesozoic (Ye, 1982; Suo et al., 2015). Owing to the intense tectonic movements, contacts between the island of Taiwan and mainland China occurred during the Late Cretaceous-Early Paleocene and Late Eocene-Early Oligocene (Teng, 1992; Zhang, 1995). One hypothesis that has been put forward is that tropical rainforests in the Indo-Malayan region may have appeared near the Cretaceous-Paleogene (K-Pg) boundary (Wang et al., 2012). Macrofossils of certain plants, closely related to present subtropical species, have been recorded from Taiwan during the Early Miocene, but pollen fossils date to the Oligocene (Li, 2000), although their geographic origins are still debated (Huang, 2011). Due to the landmass being subjected to stretching and rifting (Ye, 1982; Teng, 1992; Suo et al., 2015), part of the mountain ranges on the island of Taiwan represents a relict area of the ‘Taiwan-Sinzi Folded Zone’ (Ye, 1982; Teng, 1992; Li

and Wen, 2016), which helped facilitate an increasingly cooler climate in Asia during the Late Eocene (Zachos et al., 2001). Around this time, a vicariance event between Taiwan and mainland China may have occurred. Based on the results of our *Abelia* sequencing, the Taiwan (Yilan) flora may contain relatively ancient components (Li and Wen, 2016). The flora of mainland China has been acknowledged to have contributed to Taiwan's floristic assembly (Li and Keng, 1950). The Luzon arc did not begin to collide with the Eurasian plate until the Late Miocene (9-6 Ma) (Sibuet et al., 2002). Thus, we hypothesize that the relatively young gene flow in the flora of Taiwan may be derived from plants in mainland China, whereas the ancient components are derived solely from plants in mainland China. This hypothesis needs further validation by combining phylogenetic and molecular dating methods, as well as by studying other plant groups, particularly more ancient lineages.

The crown group of *Abelia* is dated to have formed during the late Eocene (35.07 Ma, 25.00-39.88 Ma; node 1), later than the early uplift of the Qinghai-Tibet Plateau (QTP). However, ancestral area reconstructions revealed that the *A. uniflora* complex might have colonized southwest China, Central-East China, and Taiwan during the Eocene (Fig. 8).

### *Potential Refugia and Demographic History*

Quaternary climate shifts and associated environmental changes may have made the diversification of *Abelia* relatively complicated. On one hand, diversification would have been sustained by Pleistocene glaciations because species distributions underwent expansion and contraction, leading to population migration or extinction. On the other hand, no clear geographical isolation, differentiation and subsequent population expansion (Comes et al., 2008; Qiu et al., 2011) occurred.

Our ENM analysis provides a detailed picture of the last glacial cycle (Figs. 8 and S8). The results indicate that species differentiation in *Abelia* occurred in the Oligocene, suggesting that extant populations likely differentiated well before the LGM and also provide strong evidence for survival of *Abelia* in southwest China during the LGM period (Fig. S8). Therefore, the climatic shock in the LGM may have had a significant impact on the recent

history of *Abelia* at the population level compared with the earlier period of species differentiation (Qiu et al., 2011; Qi et al., 2012). Potential suitable habitat for *A. forrestii* was distributed mainly over southwest China during the LGM period. However, its current distribution is only in Yunnan and Sichuan of southwest China from 1900 to 3300 m in altitude.

Based on genetic diversity, although the *Abelia* distribution area is highly discontinuous (Fig. 5), the populations still show similar or even higher diversity at haplotypes (nuclear data) (Table S3). *A.* × *grandiflora* has the highest genetic diversity ($\pi$=0.478), with the expected heterozygosity (*He*) ranging from 0.351-0.474 and the observed heterozygosity (*Ho*) ranging from 0.436-0.778. *Abelia schumannii* has the highest expected heterozygosity (*He*=0.474), while the highest observed heterozygosity (*Ho*=0.778) is in *A. macrotera* var. *deutziaefolia*. Based on our nuclear haplotype networks (Fig. 5), the populations of mainland China, Taiwan and Japan have significant genetic differentiation (Fig. 5). Based on ENM analysis, *A. chinensis* var. *ionandra* expanded to the coastal regions of East China and reached Taiwan via land bridges across the Taiwan Strait during the glacial period. Due to repeated glacial-interglacial cycles, mainland China and Taiwan populations may have experienced frequent gene flow through a continental bridge during the Quaternary.

Notably, we found that the populations in Jiangxi Province, which have not been dispersed to other areas, have a unique haplotype (H10, Fig. 5) and high genetic diversity (JX, $\pi$: 0.596; Table S3). After the LGM, *Abelia* populations in southeastern China may have experienced a large-scale population extinction event, and Jiangxi may be a glacial refuge for *A. chinensis*. The H13 haplotype can be found in the eastern coastal areas of China and Japan (e.g., Hubei, Taiwan and Ryukyu islands), however, no bottleneck effects (i.e., high genetic diversity and high genetic differentiation) were observed as would be expected for a refugial population (Hewitt, 2000). In addition, both the southwest and central China lineages were found to harbor the ancestral haplotype (H9). The predicted results of ENM during the LGM also support this conclusion of a refugial area (Fig. S8). The uplift of the QTP was a consequence of the collision of the Indian subcontinent with the Eurasian plate 40-50 million

years ago (Yin and Harrison, 2000; Fu et al., 2020). Because of multiple asynchronous expansions, multiple independent refugia *in situ* and complex topography in this region might explain why accurate analyses of species distribution patterns are difficult (Cun and Wang, 2010; Yan et al., 2012; Shao et al., 2015).

Our findings, together with those from other studies in this region (Han et al., 2016), suggest that, apart from geographic barriers, local adaptation to different climatic conditions appear to be the major drivers for lineage diversification of plants endemic to East Asian land-bridge islands.

## CONCLUSIONS

Robust phylogenetic relationships were consistently reconstructed within *Abelia* based on comprehensive taxon sampling, using both nuclear and plastid data. The nuclear and plastid phylogenies show that *A. schumannii* is nested within *A. macrotera*, and that *A. macrotera* var. *zabelioides* is sister to *A. uniflora*. Also, there was substantial discordance in the backbone of *Abelia*, and the network (12-sample) analyses suggested that *A chinensis*, *A. macrotera* and *A. uniflora* are all from complex hybrid origins.

We used molecular dating, biogeographic and ENM methods to explore how geology and climate together influenced the evolutionary history of *Abelia*, an ecologically sensitive and cold-adapted genus. High genetic divergences were detected among *Abelia* populations in southwest China, Central China, and Taiwan, and several interglacial refugia were recognized in the central Hengduan Mountains. Ancestral area reconstruction revealed that *Abelia* originated in southwest China, and its diversification began during the late Eocene, colonizing Central China in the mid-Oligocene, and finally dispersing to the island of Taiwan via a land bridge at approximately 19.33 Ma. Based on phylogeographic and ENM analyses, frequent gene flow might have existed between populations of mainland China and the island of Taiwan with repeated continuous dispersal between the two regions. Our research represents one of the first comprehensive phylogeographic studies investigating plant

disjunctions between the island of Taiwan and mainland China, while supporting hypotheses of postglacial range contraction together with topographic heterogeneity being responsible for the observed disjunction.

## TAXONOMIC TREATMENT

***Abelia uniflora*** R. Br. in Wall., Pl. As. Rar. 1. 15. 1830. -Type: China, Fujian, [‘Ngan-Ke-Kyen’Black Tea Country], *Reeves s.n.* (holotype CGE!, isotype BM!).

=*Abelia macrotera* (Graebn. & Buchw.) Rehder var. *zabelioides* Landrein, Kew Bull. 74(4)-70: 93. 2019. Type: China, Sichuan, Leshan Pref., E’mei Shan, 21 June 1938, *H. C. Chow 7573* (holotype A!). **Synonym nov.**

### Author contributions

H.F.W. and J.W. conceived the study. H.F.W. and D.F.M-B. performed the research and analyzed the data. Q.H.S., D.F.M-B., H.X.W., J.W. J.B.L, and H.F.W. wrote and revised the manuscript.

### ACKNOWLEDGEMENTS

The work was funded by National Science Foundation of China (31660055). We appreciate Gabriel Johnson for his help with the target enrichment experiment, and the United States National Herbarium for collection access. We acknowledge the staff in the Laboratories of Analytical Biology at the National Museum of Natural History, the Smithsonian Institution for technical support and assistance.

## REFERENCES

**Akaike H. 1998.** Information theory and an extension of the maximum likelihood principle. *Selected papers of hirotugu akaike* 199-213.

**Bell CD, Donoghue MJ. 2005.** Phylogeny and biogeography of Valerianaceae (Dipsacales) with special reference to the South American valerians. *Organisms Diversity and*

*Evolution* **5**: 147-159.

**Cao YN, Wang IJ, Chen LY, Ding YQ, Liu LX, Qiu YX. 2016.** Inferring spatial patterns and drivers of population divergence of *Neolitsea sericea* (Lauraceae), based on molecular phylogeography and landscape genomics. *Molecular Phylogenetics and Evolution* **126**: 162-172.

**Chen XD, Yang J, Feng LI, Zhou T, Zhang H, Li HM, Bai GQ, Meng X, Li ZH, Zhao GF. 2020.** Phylogeography and population dynamics of an endemic oak (Quercus fabri Hance) in subtropical China revealed by molecular data and ecological niche modeling. *Tree Genetics Genomes* **16**: 1-132.

**Chen ZD, Ying JS, Lu AM. 2012.** Disjunct distribution of seed plants between southwestern China and Taiwan Island island of China. *Chinese Journal of Botany* **47**: 551-570.

**Chou YW, Thomas PI, Ge XJ, LePage BA, Wang CN. 2011.** Refugia and phylogeography of Taiwania in East Asia. *Journal of Biogeography* **38**: 1992-2005.

**Comes HP, Tribsch A, Bittkau C. 2008.** Plant speciation in continental island floras as exemplified by *Nigella* in the Aegean Archipelago. *Philosophical Transactions of the Royal Society B: Biological Sciences* **363**: 3083-3096.

**Cun YZ, Wang XQ. 2010.** Plant recolonization in the Himalayan from the southeastern Qinghai-Tibetan Plateau: geographical isolation contributed to high population differentiation. *Molecular Phylogenetics and Evolution* **56**: 972-982.

**Degnan JH, Rosenberg NA. 2009.** Gene tree discordance, phylogenetic inference and the multispecies coalescent. *Trends in Ecology and Evolution* **24**: 332-340.

**Doyle JJ, Doyle J. 1987.** A rapid DNA isolation procedure for small quantities of fresh leaf tissue. *Phytochemical Bulletin* **19**: 11-15.

**Drummond AJ, Suchard MA, Xie D, Rambaut A. 2012.** Bayesian phylogenetics with BEAUti and the BEAST 1.7. *Molecular Biology Evolution* **29**: 1969-1973.

**Earl DA. 2012.** STRUCTURE HARVESTER: a website and program for visualizing STRUCTURE output and implementing the Evanno method. *Conservation Genetics Resources* **4**: 359-361.

**Evanno G, Regnaut S, Goudet J. 2005.** Detecting the number of clusters of individuals using the software STRUCTURE: a simulation study. *Molecular Ecology* **14**: 261-2620.

**Fu PC, Sun SS, Khan G, Dong XX, Tan JZ, Favre A, Zhang FQ, Chen SL. 2020.** Population subdivision and hybridization in a species complex of Gentiana in the Qinghai-Tibetan Plateau. *Annals of botany* **125**: 677-690.

**Foll M, Gaggiotti O. 2008.** A genome scan method to identify selected loci appropriate for both dominant and codominant markers: a Bayesian perspective. *Genetics* **180**: 977-993.

**Gan X, Stegle O, Behr J, Steffen JG, Drewe P, Hildebrand KL, Lyngsoe R, Schultheiss SJ, Osborne EJ, Sreedharan VT. 2011.** Multiple reference genomes and transcriptomes for *Arabidopsis thaliana*. *Nature* **477**: 419-423.

**Givnish TJ, Renner SS. 2004.** Tropical intercontinental disjunctions: Gondwana breakup, immigration from the boreotropics, and transoceanic dispersal. *International Journal of Plant Sciences* **165**: S1-S6.

**Grant PR, Grant BR. 2019.** Hybridization increases population variation during adaptive radiation. *Proceedings of the National Academy of Sciences* **116**: 23216-23224.

**Hahn C, Bachmann L, Chevreux B. 2013.** Reconstructing mitochondrial genomes directly from genomic next-generation sequencing reads: a baiting and iterative mapping approach. *Nucleic Acids Research* **41**: e129-e129.

**Huang S. 2011.** Historical biogeography of the flora of Taiwan. *Journal of the National Taiwan Island Museum* **64**: 33-63.

**Hoang DT, Chernomor O. 2018.** UFBoot2: improving the ultrafast bootstrap approximation. *Molecular Biology and Evolution* **35**: 518-522.

**Hodel RG, Chen SC, Payton AC, Mcdaniel SF, Soltis P, Soltis DE. 2017.** Adding loci improves phylogeographic resolution in red mangroves despite increased missing data: comparing microsatellites and RAD-Seq and investigating loci filtering. *Scientific Reports* **7**: 17598.

**Jacobs B, Pyck N, Smets E. 2010.** Phylogeny of the Linnaea clade: are *Abelia* and *Zabelia* closely related?. *Molecular Phylogenetics and Evolution* **57**: 741-752.

**Jakobsson M, Rosenberg NA. 2007.** CLUMPP: a cluster matching and permutation program for dealing with label switching and multimodality in analysis of population structure. *Bioinformatics* **23**: 1801-1806.

**Jiang XL, Hipp AL, Deng M, Su T, Zhou ZK, Yan MX. 2019.** East Asian origins of European holly oaks (*Quercus* section *Ilex* Loudon) via the Tibet□Himalaya. *Journal of Biogeography* **46**: 2203-2214.

**Jin WY, Li HW, Wei R, Huang BH, Liu B, Sun TT, Mabberley DJ, Liao PC, Yang Y. 2020.** New insights into biogeographical disjunctions between Taiwan and the Eastern Himalayas: The case of *Prinsepia* (Rosaceae). *Taxon* **69**: 278-289.

**Kalyaanamoorthy S, Minh BQ, Wong TK, Von Haeseler A, Jermiin LS. 2017.** ModelFinder: fast model selection for accurate phylogenetic estimates. *Nature Methods* **14**: 587-589.

**Katoh K, Standley DM. 2013.** MAFFT multiple sequence alignment software version 7: improvements in performance and usability. *Molecular Biology and Evolution* **30**: 772-780.

**Kim TJ, Sun BY, Park CW, Suh Y. 1998.** Phylogenetic implications of *matK* sequences in Caprifoliaceae. *American Journal of Botany* **48**: 1-48.

**Landrein S, Buerki S, Wang HF, Clarkson JJ. 2017.** Untangling the reticulate history of species complexes and horticultural breeds in *Abelia* (Caprifoliaceae). *Annals of Botany* **120**: 257-269.

**Landrein S, Farjon A. 2020.** A monograph of Caprifoliaceae: Linnaeeae. *Kew Bulletin* **74**: 1-197.

**Lanfear R, Calcott B, Ho SYW, Guindon S. 2012.** PartitionFinder: combined selection of partitioning schemes and substitution models for phylogenetic analyses. *Molecular Biology and Evolution* **29**: 1695-1701.

**Lanier HC, Knowles LL. 2012.** Is recombination a problem for species-tree analyses?.

*Systematic Biology* **61**: 691-701.

**Li J, Milne RI, Ru D, Miao J, Tao W, Zhang L, Mao K. 2000.** Allopatric divergence and hybridization within *Cupressus chengiana* (Cupressaceae), a threatened conifer in the northern Hengduan Mountains of western China. *Molecular Ecology* **29**: 1250-1266.

**Li H. 2011.** A statistical framework for SNP calling, mutation discovery, association mapping and population genetical parameter estimation from sequencing data. *Bioinformatics* **27**: 2987-2993.

**Li HL, Keng H. 1950.** Phytogeographical affinities of southern Taiwan. *Taiwania* **1**: 103-128.

**Li R, Wen J. 2016.** Phylogeny and diversification of Chinese Araliaceae based on nuclear and plastid DNA sequence data. *Journal of Systematics and Evolution* **54**: 453-467.

**Librado P, Rozas J. 2009.** DnaSP v5: a software for comprehensive analysis of DNA polymorphism data. *Bioinformatics* **25**: 1451-1452

**Liu YP, Ren ZM, Harris AJ, Peterson PM, Wen J, Su X. 2018.** Phylogeography of *Orinus* (Poaceae), a dominant grass genus on the Qingha-Tibet Plateau. *Botanical Journal of the Linnean Society* **186**: 202-223.

**Linder PH, Antonelli A, Humphreys AM, Pirie MD, Wüest RO. 2013.** What determines biogeographical ranges? Historical wanderings and ecological constraints in the danthonioid grasses. *Journal of Biogeography* **40**: 821-834.

**Link-Pérez MA, Dollo VH, Weber KM, Schussler EE. 2010.** What's in a Name: Differential labelling of plant and animal photographs in two nationally syndicated elementary science textbook series. *International Journal of Science Education* **32**: 1227-1242.

**Lu SY, Peng CI, Cheng YP, Hong KH, Chiang TY. 2001.** Chloroplast DNA phylogeography of *Cunninghamia konishii* (Cupressaceae), an endemic conifer of Taiwan. *Genome* **44**: 797-807.

**Manchester SR. 2000.** Update on the megafossil flora of Florissant, Colorado. *Denver Museum of Nature and Science* **4**:137-162.

**Morales-Briones DF, Liston A, and Tank DC. 2018.** Phylogenomic analyses reveal a deep

history of hybridization and polyploidy in the Neotropical genus *Lachemilla* (Rosaceae). New Phytologist **218**: 1668-1684.

**Morales-Briones DF, Gehrke B, Huang CH, Liston A, Ma H, Marx HE, Tank DC and Yang Y. 2021.** Analysis of paralogs in target enrichment data pinpoints multiple ancient polyploidy events in *Alchemilla* s.l. (Rosaceae). *Systematic Biology* syab032.

**Mummenhoff K, Linder P, Friesen N, Bowman JL, Lee JY, Franzke A. 2004.** Molecular evidence for bicontinental hybridogenous genomic constitution in *Lepidium* sensu stricto (Brassicaceae) species from Australia and New Zealand. *American Journal of Botany* **91**: 254-261.

**Nathan R, Schurr FM, Spiegel O, Steinitz O, Trakhtenbrot A, Tsoar A. 2008.** Mechanisms of long-distance seed dispersal. *Trends in ecology evolution* **23**: 638-647.

**Nguyen LT, Schmidt HA, von Haeseler A, Minh, BQ. 2015.** IQ-TREE: a fast effective stochastic algorithm for estimating maximum-likelihood phylogenies. *Molecular Biology and Evolution* **32**: 268-274.

**Nie ZL, Sun H, Li H, Wen J. 2007.** Intercontinental biogeography of subfamily Orontioideae (*Symplocarpus*, *Lysichiton*, and *Orontium*) of Araceae in eastern Asia and North America. *Molecular Phylogenetics and Evolution* **40**: 155-165.

**Niu YT, Ye JF, Zhang JL, Wan JZ, Yang T, Wei XX, Lu LM, Li JH, Chen ZD. 2018.** Long-distance dispersal or postglacial contraction? Insights into disjunction between Himalayan-Hengduan Mountains and Taiwan Island in a cold-adapted herbaceous genus, *Triplostegia*. *Ecology and Evolution* **8**: 1131-1146.

**Nosil P. 2008.** Speciation with gene flow could be common. *Molecular ecology* **1**7: 2103-2106.

**Nwankwo EC, Mortega KG, Karageorgos A, Ogolowa BO, Papagregoriou G, Grether GF, Ara Monadjem, Kirschel AN. 2019.** Rampant introgressive hybridization in *Pogoniulus* tinkerbirds (Piciformes: Lybiidae) despite millions of years of divergence. *Biological Journal of the Linnean Society* **127**: 125-142.

**Nylander JAA, Ronquist F, Huelsenbeck JP, Nieves-Aldrey JL. 2004.** Bayesian phylogenetic analysis of combined data. *Systematic Biology* **53**: 47-67.

**Peakall R, Smouse PE. 2006.** GENALEX 6: genetic analysis in Excel. Population genetic software for teaching and research. *Molecular Ecology Notes* **6**: 288-295.

**Phillips SJ, Anderson RP, Schapire RE. 2006.** Maximum entropy modeling of species geographic distributions. *Ecological Modelling* **190**: 231-259.

**Pritchard JK, Stephens M, Donnelly P. 2000.** Inference of population structure using multilocus genotype data. *Genetics* **155**: 945-959.

**Qian H, Ricklefs RE. 2004.** Geographical distribution and ecological conservatism of disjunct genera of vascular plants in eastern Asia and eastern North America. *Journal of Ecology* **92**: 253-265.

**Qiu YX, Fu CX, Comes HP, 2011.** Plant molecular phylogeography in China and adjacent regions: Tracing the genetic imprints of Quaternary climate and environmental change in the world's most diverse temperate flora. *Molecular Phylogenetics and Evolution* **59**: 225-244.

**Qiu YX, Guan BC, Comes HP. 2009a.** Did glacials and/or interglacials promote allopatric incipient speciation in East Asia temperate plants? Phylogeographic and coalescent analyses on refugial isolation and divergence in Dysosma versipellis. *Molecular Phylogenetics and Evolution* **51**: 281-293.

**Rambaut A, Suchard MA, Xie D, Drummond AJ. 2014.** Tracer, version 1.6. http://beast.bio.ed.ac.uk/Tracer/

**Rendón-Anaya M, Ibarra-Laclette E, Méndez-Bravo L, Lan T, Zheng C, Carretero-Paulet L, Herrera-Estrella L. 2019.** The avocado genome informs deep angiosperm phylogeny, highlights introgressive hybridization, and reveals pathogen-influenced gene space adaptation. *Proceedings of the National Academy of Sciences* **116**: 17081-17089.

**Rieseberg LH, Carney SE.1998.** Tansley review no. 102 Plant hybridisation. *New Phytol* **140**: 599-624.

**Šarhanová P, Sharbel TF, Sochor M, Vašut RJ, Dančák M and Trávníček B. 2017.**

Hybridization drives evolution of apomicts in *Rubus* subgenus *Rubus*: evidence from microsatellite markers. *Annals of Botany* **120**: 317-328.

**Schwarz G. 1978.** Estimating the dimension of a model. *Annals of Statistics* **6**: 461-464

**Shao YZ, Chen Y, Zhang XC, Xiang QP. 2015.** Species delimitation and phylogeography of the *Abies chensiensis* complex inferred from morphological and molecular data. *Botanical Journal of the Linnean Society* **177**: 175-188.

**Shi Y, Cui Z, Su Z. 2006.** The Quaternary glaciations and environmental variations in China. *Hebei Science and Technology Press* **65**: 101.

**Sibuet JC, Hsu SK, Le Pichon X, Le Formal JP, Reed D, Morre G, Liu CS. 2002.** East Asia plate tectonics since 15 Ma: constraints from the Taiwan Island region. *Tectonophysics* **344**: 103-134.

**Sibuet JC, Hsu SK. 2004.** How was Taiwan Island created?. *Tectonophysics* **379**: 159-181.

**Smith SA, Dunn CW. 2008.** Phyutility: a phyloinformatics tool for trees, alignments and molecular data. *Bioinformatics* **24**: 715-716.

**Sugiura N. 1978.** Further Analysis of the Data by Akaike's Information Criterion and the Finite Corrections. *Communications in Statistics-Theory and Methods* **7**: 13-26.

**Suo YH, Li SZ, Zhao SJ, Somerville ID, Yu S, Dai LM, Xu LQ, Cao XZ, Wang PC. 2015.** Continental margin basins in East Asia: tectonic implications of the Meso- Cenozoic East China Sea pull-apart basins. *Geological Journal* **50**: 139-156.

**Swets JA. 1988.** Measuring the accuracy of diagnostic systems. *Science* **240**: 1285-1293.

**Teng LS. 1992.** Geotectonic evolution of Tertiary continental margin basins of Taiwan. *Petroleum Geology of Taiwan Island* **27**: 1-19.

**Vargas OM, Heuertz M, Smith SA, Dick CW. 2019.** Target sequence capture in the Brazil nut family (Lecythidaceae): Marker selection and in silico capture from genome skimming data. *Molecular Phylogenetics and Evolution* **135**: 98-104.

**Wallich N. 1829.** *Plantae Asiaticae rariores*. London, Paris, Strasburgh: Treuttel and Würtz

**Wang HF, Landrein S, Dong WP, Nie ZL, Kondo K, Funamoto T, Wen J, Zhou SL. 2015.**

Molecular phylogeny and biogeographic diversification of Linnaeoideae (*Carprifoliaceae s.l.*) disjunctively distributed in Eurasia, North American and Mexico. *PLoS One* **10**: e0116485.

**Wang HX, Liu H, Moore MJ, Landrein S, Liu B, Zhu ZX, Wang HF. 2020.** Plastid phylogenomic insights into the evolution of the Caprifoliaceae *s.l.* (Dipsacales). *Molecular Phylogenetics and Evolution* **142**: 106641.

**Wang HX, Morales-Brionesb DF, Moorec MJ, Wen J, Wang HF. 2021.** A phylogenomic perspective on gene tree conflict and character evolution in *Caprifoliaceae* using target enrichment data, with Zabelioideae recognized as a new subfamily. *Journal of Systematics and Evolution* https://doi.org/10.1111/jse.12745.

**Wang IJ. 2013.** Examining the full effects of landscape heterogeneity on spatial genetic variation: a multiple matrix regression approach for quantifying geographic and ecological isolation. *Evolution* **67**: 3403-3411.

**Wang J, Feng C, Jiao T, Von Wettberg EB, Kang M. 2017.** Genomic Signature of Adaptive Divergence despite Strong Nonadaptive Forces on Edaphic Islands: A Case Study of *Primulina juliae*. *Genome Biology and Evolution* **9**: 3495-3508.

**Wang W, Ortiz RDC, Jacques FM, Xiang XG, Li H., Lin L, Chen ZD. 2012.** Menispermaceae and the diversification of tropical rainforests near the Cretaceous-Paleogene boundary. *New Phytologist* **195**: 470-478.

**Wang Z, Liu KJ. 2016.** A performance study of the impact of recombination on species tree analysis. *BMC Genomics* **17**: 165-174.

**Wei XX, Yang ZY, Li Y, Wang XQ. 2010.** Molecular phylogeny and biogeography of Pseudotsuga (Pinaceae): insights into the floristic relationship between Taiwan Island and its adjacent areas. *Molecular Phylogenetics and Evolution* **55**: 776-785.

**Weitemier K, Straub SCK, Cronn RC, Fishbein M, Schmickl R, McDonnell A, Liston A. 2014.** Hyb-Seq: combining target enrichment and genome skimming for plant phylogenomics. *Applications in Plant Sciences* **2**: 1400042.

**Wen J. 2001.** Evolution of eastern Asian-eastern North American biogeographic disjunctions: a few additional issues. *International Journal of Plant Sciences* **162**: S117-S122.

**Wen J, Nie ZL, Ickert□Bond SM. 2018.** Advances in biogeography in the age of a new modern synthesis. *Journal of Systematics and Evolution* **57**: 543-546.

**Wen J, Ree RH, Ickert-Bond SM, Nie Z, Funk V. 2013.** Biogeography: where do we go from here?. *Taxon* **62**: 912-927.

**Wen J, Wagner WL. 2020.** Collections-based systematics and biogeography in the 21st century. *Journal of Systematics and Evolution* **58**: 743-750.

**Wu PC, Wang MZ. 2001.** Relationship of the tropical elements of the bryophytes between Hengduan Mts., southwest China and Taiwan Island province, southeast China. *Guizhou Science* **19**: 6-9.

**Xiang CL, Dong HJ, Landrein S, Zhao F, Yu WB, Soltis DE, Peng H. 1998.** Revisiting the phylogeny of Dipsacales: new insights from phylogenomic analyses of complete plastomic sequences. *Journal of Systematics and Evolution* **58**: 103-117.

**Xiang KL, Zhao L, Erst AS, Yu SX, Jabbour F, Wang W. 2017.** A molecular phylogeny of *Dichocarpum* (Ranunculaceae): Implications for eastern Asian biogeography. *Molecular Phylogenetics and Evolution* **107**: 594-604.

**Xiang QY, Soltis DE. 2001.** Dispersal-vicariance analyses of intercontinental disjuncts: historical biogeographical implications for angiosperms in the Northern Hemisphere. *International Journal of Plant Sciences* **162**: S29-S39.

**Xu J, Deng M, Jiang XL, Westwood M, Song YG, Turkington R. 2015.** Phylogeography of *Quercus glauca* (Fagaceae), a dominant tree of East Asian subtropical evergreen forests, based on three chloroplast DNA interspace sequences. *Tree Genet Genomes* **11**: 805.

**Yan HF, Zhang CY, Wang FY, Hu, CM, Ge XJ, Hao G. 2012.** Population expanding with the phalanx model and lineages split by environmental heterogeneity: a case study of *Primula obconica* in subtropical China. *PLoS One* **7**: e41315.

**Yang Q, Landrein S. 2011.** *Linnaeaceae*. *Flora of China* **19**: 642-648.

**Yang Y, Smith SA. 2014.** Orthology inference in nonmodel organismsusing transcriptomes and low-coverage genomes: improving accuracy and matrix occupancy for phylogenomics. *Molecular Biology and Evolution* **31**: 3081-3092.

**Ye J, Lu L, Liu B, Yang T, Zhang J, Hu H, Chen Z. 2019.** Phylogenetic delineation of regional biota: A case study of the Chinese flora. *Molecular Phylogenetics and Evolution* **135**: 222-229.

**Ye XQ. 1982.** On the formation and development of the geology and geomorphology of Taiwan. *Journal Central China Teachers College* 83-89.

**Ye XY, Ma PF, Yang GQ, Guo C, Zhang YX, Chen YM, Li DZ. 2019.** Rapid diversification of alpine bamboos associated with the uplift of the Hengduan Mountains. *Journal of Biogeography* **46**: 2678-2689.

**Ye Z, Zhu G, Chen P, Zhang D, Bu W. 2014.** Molecular data and ecological niche modelling reveal the Pleistocene history of a semi-aquatic bug (*Microvelia douglasi douglasi*) in East Asia. *Molecular Ecology* **23**: 3080-3096.

**Yin A, Harrison TM. 2000.** Geologic evolution of the Himalayan Tibetan orogen. *Annual Review of Earth and Planetary Sciences* **28**: 211-280.

**Yoder AD, Nowak MD. 2006.** Has vicariance or dispersal been the predominant biogeographic force in Madagascar? Only time will tell. *Ecology Evolution and Systematics* **37**: 405-431.

**Yu Y, Harris AJ, Blair C, He X. 2015.** RASP (Reconstruct Ancestral State in Phylogenies): a tool for historical biogeography. *Molecular Phylogenetics and Evolution* **87**: 46-49.

**Zachos J, Pagani M, Sloan L, Thomas E, Billups K. 2001.** Trends, rhythms, and aberrations in global climate 65 Ma to present. *Science* **292**: 686-693.

**Zhang C, Rabiee M, Sayyari E, Mirarab S. 2018.** ASTRAL-III: polynomial time species tree reconstruction from partially resolved gene trees. *BMC Bioinformatics* **19**: 15-30.

## Figure Legends

Figure 1. Photographs of *Abelia* taxa. (A) *A. chinensis*; (B) *A. chinensis* var. *ionandra*; (C) *A.*

*forrestii*;(D) *A.* × *grandiflora*; (E) *A.* × *grandiflora* 'Francis Mason'; (F) *A. macrotera*; (G) *A. macrotera* var. *macrotera*; (H) *A. uniflora*; (I) *A. schumannii.*

Figure 2. Tanglegram of the nuclear concatenated (left) and plastid (right) phylogenies. Dotted lines connect taxa between the two phylogenies. Maximum likelihood bootstrap support values are shown above branches. The asterisks indicate maximum likelihood bootstrap support of 100%. Major taxonomic groups or main clades in the family as currently recognized are indicated by branch colors as a visual reference to relationships.

Figure 3. ASTRAL-III species tree; Clade support is depicted as: Quartet Concordance (QC)/Quartet Differential (QD)/Quarte Informativeness (QI)/Local posterior probabilities (LPP).

Figure 4. Best supported species networks inferred with PhyloNet for the (A) 15 samples, (B) 12 samples. Numbers next to the inferred hybrid branches indicate inheritance probabilities. Red lines represent minor hybrid edges (edges with an inheritance contribution < 0.50).

Figure 5. Distribution of 12 Hyb-seq haplotypes in *Abelia.* (A) Geographical distribution of haplotypes among four *Abelia* species, (B) The network of 15 chloroptypes, (C) Results of STRUCTURE analysis for all individuals of *Abelia* studied based on *Fst* data.

Figure 6. BEAST analysis of divergence times based on nuclear data. Calibration points are indicated by A, B. Numbers 1-13 represent major divergence events in *Abelia*; mean divergence times and 95% highest posterior densities are provided for each.

Figure 7. Ancestral area reconstruction for *Abelia*. Areas of endemism are as follows: (A) Southwest China, (B) Central-East China, (C) Taiwan and Ryukyu Islands. The numbered nodes represent crown nodes of important colonization events.

Figure 8. Comparison of potential distributions as probability of occurrence for *A. chinensis*, and *A. uniflora* at the CCSM climatic scenarios of the Last Glacial Maximum (LGM, ca. 21,000 years BP). The maximum training sensitivity plus specificity logistic threshold has been used to discriminate between suitable (cutline 0.1-1 areas) and unsuitable habitat. The darker color indicates a higher probability of occurrence.

Fig. S1 Heatmaps showing gene recovery efficiency for the nuclear gene in 45 species of *Abelia*. Columns represent genes, and each row is one accession. Shading indicates the percentage of the reference locus length coverage.

Fig. S2 Nuclear concatenated RAxML tree; Clade support is depicted as: Quartet Concordance (QC)/Quartet Differential (QD)/Quarte Informativeness (QI).

Fig. S3 Plastid RAxML tree; Clade support is depicted as: Quartet Concordance (QC)/Quartet Differential (QD)/Quarte Informativeness (QI)/Local posterior probabilities (LPP).

Fig. S4 Best species networks of the selective nuclear data estimated with PhyloNet for the 15-sample data set. A: One hybridization event; B: Two hybridization events; C: Three hybridization events; D: Four hybridization events; E: Five hybridization events. Blue branches connect the hybrid nodes. Numbers next to blue branches indicate inheritance probabilities.

Fig. S5 Best species networks of the selective nuclear data estimated with PhyloNet for the 12-sample data set. A: One hybridization event; B: Two hybridization events; C: Three hybridization events; D: Four hybridization events; E: Five hybridization events. Blue branches connect the hybrid nodes. Numbers next to blue branches indicate inheritance probabilities.

Fig. S6 Corresponding value of *Fst*.

Fig. S7. BEAST analysis of divergence times based on the plastid matrix. Calibration points are indicated by A, B. Numbers 1-8 represent major divergence events in *Abelia*; mean divergence times and 95% highest posterior densities are provided for each.

Fig. S8 Potential distribution probability (in logistic value) of occurrence for *Abelia* in East Asia generated form MAXENT.

Table. S1 The 19 bioclimatic variables for ENM analyses

Table. S2 HybPiper assembly statistics.

Table. S3 Summary of genetic diversity of *Abelia.*

970 **Table 1. List of species and vouchers used in this study.**

| Order | Ingroup/ Outgroup | Taxon | Coding | Locality | Voucher specimen number | SRA accession |
|---|---|---|---|---|---|---|
| 1 | Ingroup | *Abelia chinensis* | B | Jiujiang, Jiangxi, China | HUTB, E119 | SRR13890741 |
| 2 | Ingroup | *Abelia chinensis* | B | Jiujiang, Jiangxi, China | HUTB, E111 | SRR13890742 |
| 3 | Ingroup | *Abelia chinensis* | B | Jiujiang, Jiangxi, China | HUTB, E206 | SRR13705765 |
| 4 | Ingroup | *Abelia chinensis* var. *ionandra* | C | Keelung Islet,Taiwan, China | HUTB, E30 | SRR13705776 |
| 5 | Ingroup | *Abelia chinensis* var. *ionandra* | C | Amami Islands, Japan | HUTB, E33 | SRR13890725 |
| 6 | Ingroup | *Abelia chinensis* var. *ionandra* | C | Okinawa Island, Okinawa, Japan | HUTB, E166 | SRR13890726 |
| 7 | Ingroup | *Abelia chinensis* var. *ionandra* | C | Yilan, Taiwan, China | HUTB, E167 | SRR13890744 |
| 8 | Ingroup | *Abelia chinensis* var. *ionandra* | C | Yilan,Taiwan, China | HUTB, E229 | SRR13890743 |
| 9 | Ingroup | *Abelia chinensis* var. *ionandra* | C | Yilan, Taiwan, China | HUTB, E230 | SRR13890751 |
| 10 | Ingroup | *Abelia chinensis* var. *ionandra* | C | Yilan, Taiwan, China | HUTB, E231 | SRR13890745 |
| 11 | Ingroup | *Abelia forrestii* | A | Nujiang, Yunnan, China | HUTB, E36 | SRR13890748 |
| 12 | Ingroup | *Abelia forrestii* | A | Nujiang, Yunnan, China | HUTB, E37 | SRR13705787 |
| 13 | Ingroup | *Abelia grandiflora* | B | Zhengzhou, Henan, China | HUTB, E159 | SRR13890724 |
| 14 | Ingroup | *Abelia grandiflora* | B | Zhengzhou, Henan, China | HUTB, E227 | SRR13890730 |
| 15 | Ingroup | *Abelia macrotera* var. *mairei* | A | Emei, Sichuan, China | HUTB, E110 | SRR13705799 |
| 16 | Ingroup | *Abelia macrotera* var. *deutziaefolia* | A | Fuyang, Guizhou, China | HUTB, E153 | SRR13890758 |
| 17 | Ingroup | *Abelia macrotera* var. *deutziaefolia* | A | Fuyang, Guizhou, China | HUTB, E154 | SRR13890757 |
| 18 | Ingroup | *Abelia macrotera* var. *deutziaefolia* | A | Fuyang,Guizhou, China | HUTB, E155 | SRR13890727 |
| 19 | Ingroup | *Abelia macrotera* var. *deutziaefolia* | A | Fuyang, Guizhou, China | HUTB, E156 | SRR13890731 |
| 20 | Ingroup | *Abelia macrotera* var. *deutziaefolia* | A | Fuyang, Guizhou, China | HUTB, E157 | SRR13890728 |
| 21 | Ingroup | *Abelia macrotera* var. *deutziaefolia* | A | Fuyang, Guizhou, China | HUTB, E158 | SRR13890729 |
| 22 | Ingroup | *Abelia macrotera* var. *engleriana* | A | Nanchuan, Chongqing, China | HUTB, E34 | SRR13890756 |
| 23 | Ingroup | *Abelia macrotera* var. *engleriana* | A | Nanchuan, Chongqing, China | HUTB, E149 | SRR13890753 |
| 24 | Ingroup | *Abelia macrotera* var. *engleriana* | A | Nanchuan, Chongqing, China | HUTB, E347 | SRR13890755 |
| 25 | Ingroup | *Abelia macrotera* var. *engleriana* | A | Nanchuan, Chongqing, China | HUTB, E349 | SRR13890754 |

| | | | | | | |
|---|---|---|---|---|---|---|
| 26 | Ingroup | *Abelia macrotera* var. *zabelioides* | A | Emei, Sichuan, China | HUTB, E3 | SRR13890733 |
| 27 | Ingroup | *Abelia macrotera* var. *zabelioides* | A | Emei, Sichuan, China | HUTB, E43 | SRR13890740 |
| 28 | Ingroup | *Abelia macrotera* var. *zabelioides* | A | Emei, Sichuan, China | HUTB, E211 | SRR13890732 |
| 29 | Ingroup | *Abelia macrotera* var. *macrotera* | A | Yichang, Hubei, China | HUTB, E6 | SRR13890752 |
| 30 | Ingroup | *Abelia macrotera* var. *macrotera* | A | Yichang, Hubei, China | HUTB, E45 | SRR13890750 |
| 31 | Ingroup | *Abelia uniflora* | B | Wuyishan, Fujian, China | HUTB, E46 | SRR13890738 |
| 32 | Ingroup | *Abelia uniflora* | B | Wuyishan, Fujian, China | HUTB, E47 | SRR13890739 |
| 33 | Ingroup | *Abelia uniflora* | B | Wuyishan, Fujian, China | HUTB, E48 | SRR13890734 |
| 34 | Ingroup | *Abelia uniflora* | B | Wuyishan, Fujian, China | HUTB, E51 | SRR13705798 |
| 35 | Ingroup | *Abelia uniflora* | B | Wuyishan, Fujian, China | HUTB, E52 | SRR13890736 |
| 36 | Ingroup | *Abelia uniflora* | B | Wuyishan, Fujian, China | HUTB, E53 | SRR13890735 |
| 37 | Ingroup | *Abelia uniflora* | B | Wuyishan, Fujian, China | HUTB, E54 | SRR13890737 |
| 38 | Ingroup | *Abelia schumannii* | A | Ganzi, Sichuan, China | HUTB, E44 | SRR13890749 |
| 39 | Outgroup | *Diabelia serrata* | | Takakuma, Kagoshima, Japan | HUTB, E321 | SRR13890747 |
| 40 | Outgroup | *Diabelia sanguinea* | | Numadzu, Shizuoka, Japan | HUTB, E303 | SRR13890746 |
| 41 | Outgroup | *Dipelta floribunda* | | Cambridge, UK. | HUTB, E55 | SRR13705794 |
| 42 | Outgroup | *Dipelta floribunda* | | Cambridge, UK. | HUTB, E56 | SRR13705795 |
| 43 | Outgroup | *Kolkwitzia amabilis* | | Weinan, Shanxi, China | HUTB, E9 | SRR13705797 |
| 44 | Outgroup | *Linnaea borealis* | | Yili, Xinjiang, China | HUTB, E14 | SRR13705786 |
| 45 | Outgroup | *Vesalea occidentalis* | | Durango, Mexico | HUTB, E96 | SRR13705793 |

**Table 2. Dataset statistics, including the number of samples, number of characters, number of PI characters, missing data.**

| Alignment | No. of samples | No. sites | Missing data (%) | No. of variable/Parsimony informative sites |
|---|---|---|---|---|
| Nuclear | 45 | 365,330 | 16.88 | 43,248/22,045 |
| Plastid | 45 | 163,130 | 4.35 | 7,926/3,850 |

**Table 3. Model selection of the different species networks and bifurcating trees.**

| Topology | lnL | Parameters | Loci | Number of hybridizations | Information criteria | | |
|---|---|---|---|---|---|---|---|
| | | | | | AIC | AICc | BIC |
| **15 samples** | | | | | | | |
| nuclear ASTRAL | -4177.949631 | 27 | 167 | N/A | 8409.899262 | 8420.776960 | 8494.085095 |
| nuclear RAxML | -4148.054160 | 27 | 167 | N/A | 8350.108319 | 8360.986017 | 8434.294152 |
| Plastid | -4231.190608 | 27 | 167 | N/A | 8516.381215 | 8527.258913 | 8600.567048 |
| Network 1 | -4088.228145 | 29 | 167 | 1 | 8234.456290 | 8247.157020 | 8324.878111 |
| Network 2 | -4050.799135 | 31 | 167 | 2 | 8163.598270 | 8178.294566 | 8260.256078 |
| Network 3 | -3948.351402 | 33 | 167 | 3 | 7962.702804 | 7979.574984 | 8065.596600 |
| **Network 4** | **-3932.455932** | **35** | **167** | **4** | **7934.911864** | **7954.148505** | **8044.041647** |
| Network 5 | -3935.844300 | 37 | 167 | 5 | 7945.688601 | 7967.487050 | 8061.054372 |
| **12 samples** | | | | | | | |
| nuclear ASTRAL | -2716.350474 | 21 | 162 | N/A | 5474.700949 | 5481.300949 | 5539.540472 |
| nuclear RAxML | -2724.448876 | 21 | 162 | N/A | 5490.897753 | 5497.497753 | 5555.737276 |
| Plastid | -2723.043552 | 21 | 162 | N/A | 5488.087104 | 5494.687104 | 5552.926627 |
| Network1 | -2660.433072 | 23 | 162 | 1 | 5366.866143 | 5374.866143 | 5437.880859 |
| Network2 | -2601.023466 | 25 | 162 | 2 | 5252.046932 | 5261.605756 | 5329.236841 |
| **Network3** | **-2549.319250** | **27** | **162** | **3** | **5152.638500** | **5163.922082** | **5236.003601** |
| Network4 | -2552.995453 | 27 | 162 | 3 | 5159.990906 | 5171.274488 | 5243.356007 |
| Network 5 | -2606.591029 | 27 | 162 | 3 | 5267.182058 | 5278.465640 | 5350.547159 |

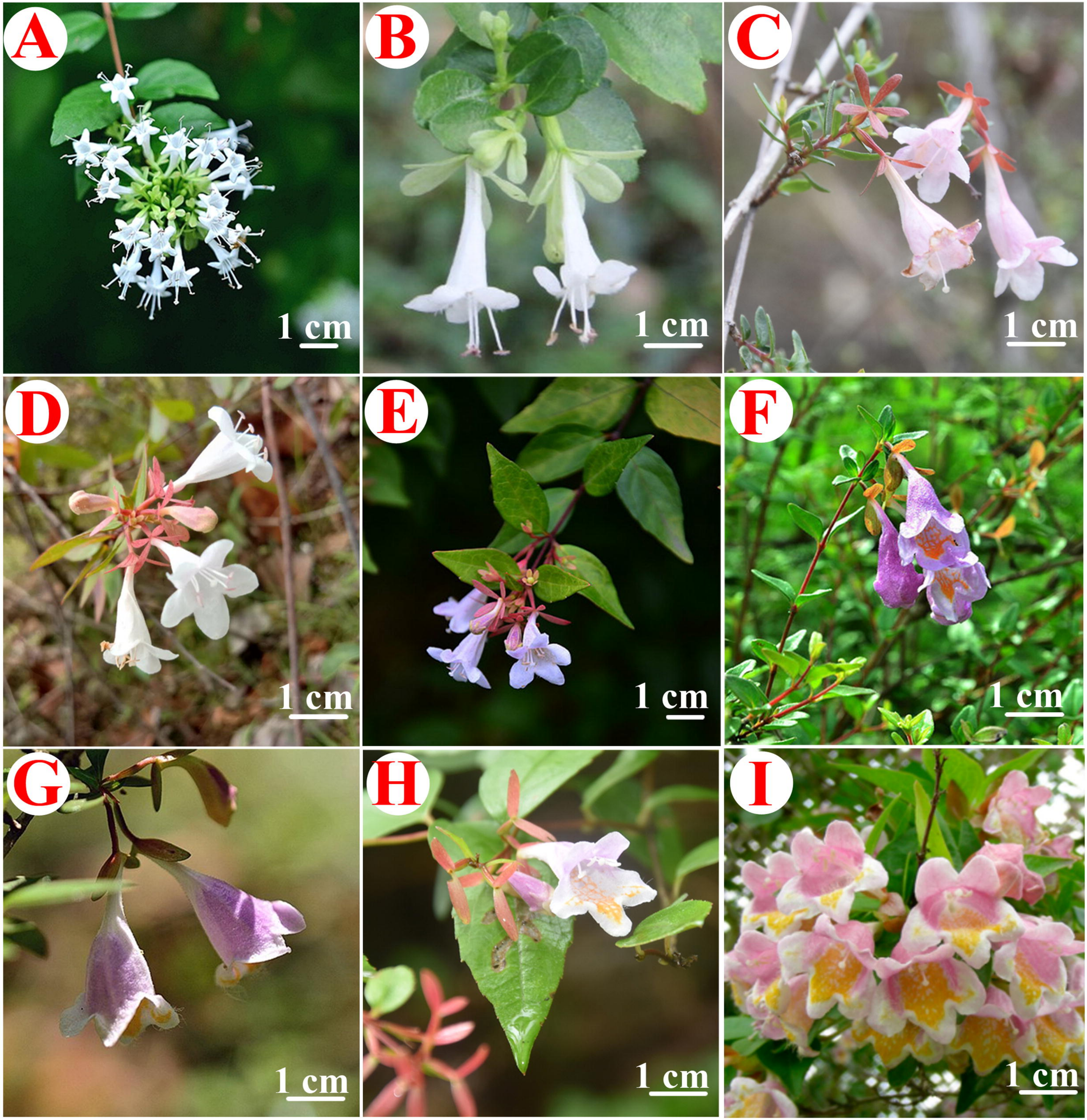
A
1 cm
B
1 cm
C
1 cm
D
1 cm
E
1 cm
F
1 cm
G
1 cm
H
1 cm
I
1 cm

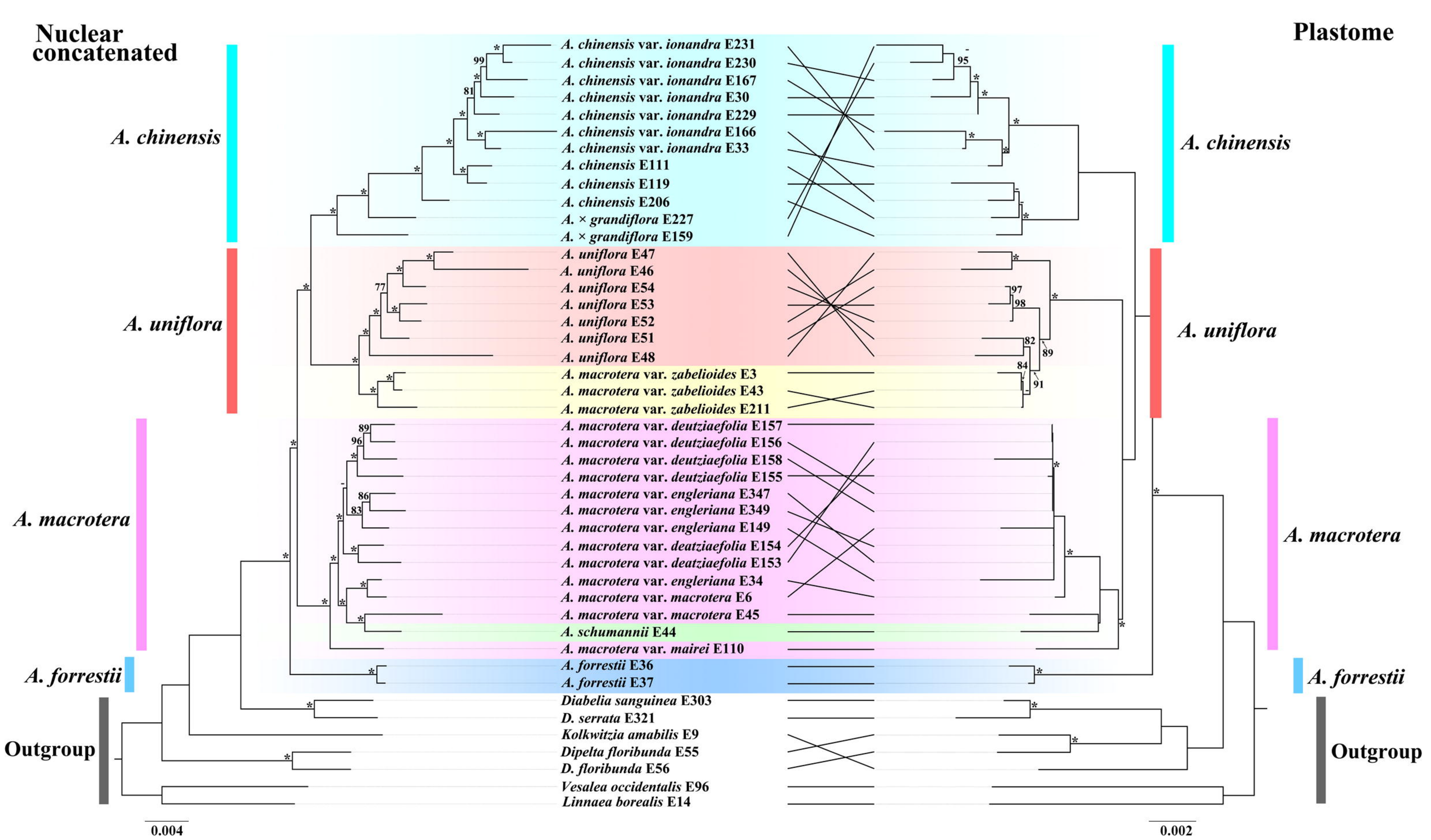
Nuclear concatenated
Plastome
A. chinensis
A. uniflora
A. macrotera
A. forrestii
Outgroup
A. chinensis var. ionandra E231
A. chinensis var. ionandra E230
A. chinensis var. ionandra E167
A. chinensis var. ionandra E30
A. chinensis var. ionandra E229
A. chinensis var. ionandra E166
A. chinensis var. ionandra E33
A. chinensis E111
A. chinensis E119
A. chinensis E206
A. × grandiflora E227
A. × grandiflora E159
A. uniflora E47
A. uniflora E46
A. uniflora E54
A. uniflora E53
A. uniflora E52
A. uniflora E51
A. uniflora E48
A. macrotera var. zabelioides E3
A. macrotera var. zabelioides E43
A. macrotera var. zabelioides E211
A. macrotera var. deutziaefolia E157
A. macrotera var. deutziaefolia E156
A. macrotera var. deutziaefolia E158
A. macrotera var. deutziaefolia E155
A. macrotera var. engleriana E347
A. macrotera var. engleriana E349
A. macrotera var. engleriana E149
A. macrotera var. deatziaefolia E154
A. macrotera var. deatziaefolia E153
A. macrotera var. engleriana E34
A. macrotera var. macrotera E6
A. macrotera var. macrotera E45
A. schumannii E44
A. macrotera var. mairei E110
A. forrestii E36
A. forrestii E37
Diabelia sanguinea E303
D. serrata E321
Kolkwitzia amabilis E9
Dipelta floribunda E55
D. floribunda E56
Vesalea occidentalis E96
Linnaea borealis E14
0.004
0.002

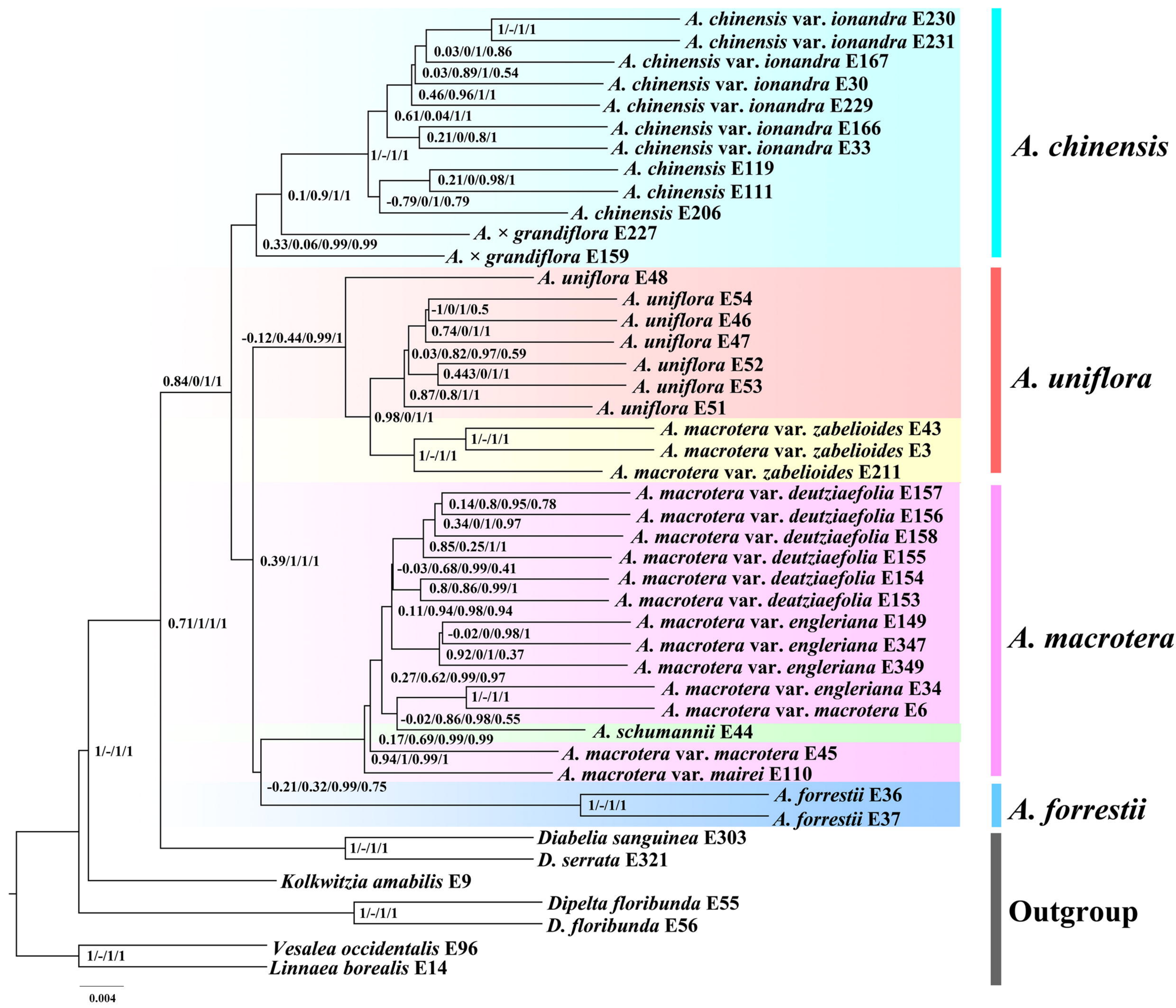
A. chinensis var. ionandra E230
A. chinensis var. ionandra E231
A. chinensis var. ionandra E167
A. chinensis var. ionandra E30
A. chinensis var. ionandra E229
A. chinensis var. ionandra E166
A. chinensis var. ionandra E33
A. chinensis E119
A. chinensis E111
A. chinensis E206
A. × grandiflora E227
A. × grandiflora E159
A. uniflora E48
A. uniflora E54
A. uniflora E46
A. uniflora E47
A. uniflora E52
A. uniflora E53
A. uniflora E51
A. macrotera var. zabelioides E43
A. macrotera var. zabelioides E3
A. macrotera var. zabelioides E211
A. macrotera var. deutziaefolia E157
A. macrotera var. deutziaefolia E156
A. macrotera var. deutziaefolia E158
A. macrotera var. deutziaefolia E155
A. macrotera var. deatziaefolia E154
A. macrotera var. deatziaefolia E153
A. macrotera var. engleriana E149
A. macrotera var. engleriana E347
A. macrotera var. engleriana E349
A. macrotera var. engleriana E34
A. macrotera var. macrotera E6
A. schumannii E44
A. macrotera var. macrotera E45
A. macrotera var. mairei E110
A. forrestii E36
A. forrestii E37
Diabelia sanguinea E303
D. serrata E321
Kolkwitzia amabilis E9
Dipelta floribunda E55
D. floribunda E56
Vesalea occidentalis E96
Linnaea borealis E14
1/-/1/1
0.03/0/1/0.86
0.03/0.89/1/0.54
0.46/0.96/1/1
0.61/0.04/1/1
0.21/0/0.8/1
1/-/1/1
0.21/0/0.98/1
-0.79/0/1/0.79
0.1/0.9/1/1
0.33/0.06/0.99/0.99
-1/0/1/0.5
0.74/0/1/1
-0.12/0.44/0.99/1
0.03/0.82/0.97/0.59
0.443/0/1/1
0.87/0.8/1/1
0.84/0/1/1
0.98/0/1/1
1/-/1/1
1/-/1/1
0.14/0.8/0.95/0.78
0.34/0/1/0.97
0.85/0.25/1/1
0.39/1/1/1
-0.03/0.68/0.99/0.41
0.8/0.86/0.99/1
0.11/0.94/0.98/0.94
0.71/1/1/1
-0.02/0/0.98/1
0.92/0/1/0.37
0.27/0.62/0.99/0.97
1/-/1/1
-0.02/0.86/0.98/0.55
0.17/0.69/0.99/0.99
1/-/1/1
0.94/1/0.99/1
-0.21/0.32/0.99/0.75
1/-/1/1
1/-/1/1
1/-/1/1
1/-/1/1
0.004
A. chinensis
A. uniflora
A. macrotera
A. forrestii
Outgroup

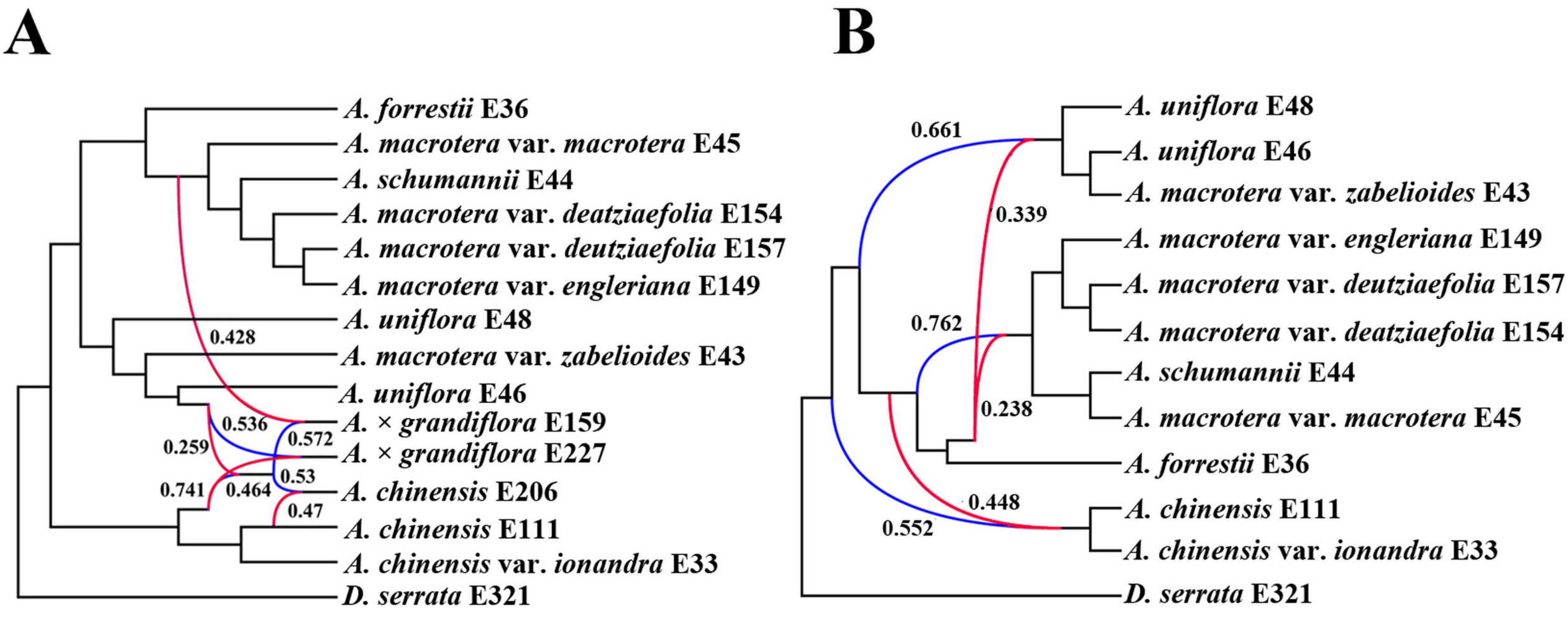
A
A. forrestii E36
A. macrotera var. macrotera E45
A. schumannii E44
A. macrotera var. deatziaefolia E154
A. macrotera var. deutziaefolia E157
A. macrotera var. engleriana E149
A. uniflora E48
A. macrotera var. zabelioides E43
A. uniflora E46
A. × grandiflora E159
A. × grandiflora E227
A. chinensis E206
A. chinensis E111
A. chinensis var. ionandra E33
D. serrata E321
0.428
0.536
0.572
0.259
0.53
0.741
0.464
0.47
B
A. uniflora E48
A. uniflora E46
A. macrotera var. zabelioides E43
A. macrotera var. engleriana E149
A. macrotera var. deutziaefolia E157
A. macrotera var. deatziaefolia E154
A. schumannii E44
A. macrotera var. macrotera E45
A. forrestii E36
A. chinensis E111
A. chinensis var. ionandra E33
D. serrata E321
0.661
0.339
0.762
0.238
0.448
0.552

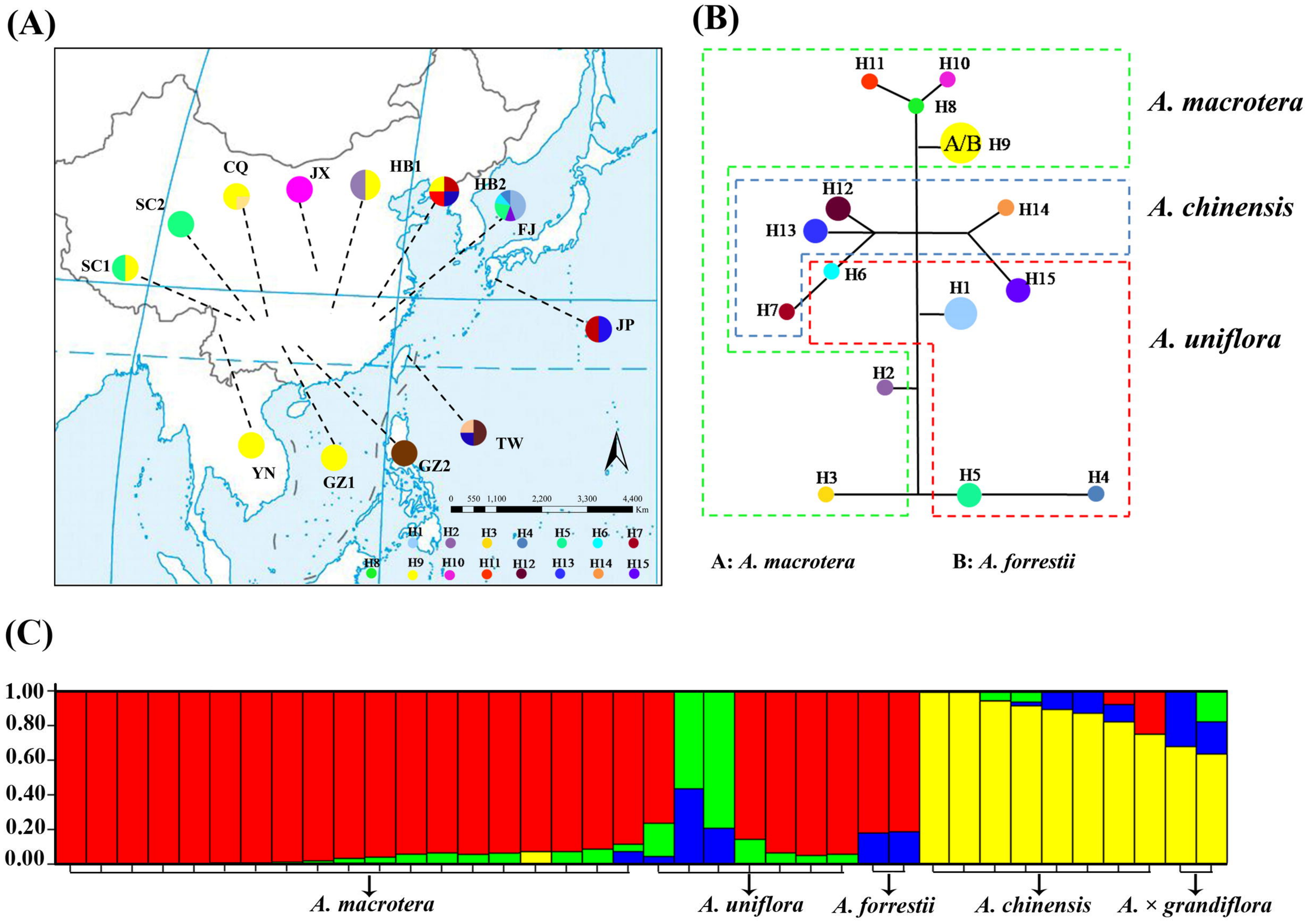
(A)
CQ
JX
HB1
HB2
SC2
FJ
SC1
JP
TW
YN
GZ1
GZ2
0 550 1,100 2,200 3,300 4,400 Km
H1 H2 H3 H4 H5 H6 H7
H8 H9 H10 H11 H12 H13 H14 H15
(B)
H11
H10
H8
A/B H9
H12
H14
H13
H6
H15
H1
H7
H2
H3
H5
H4
A. macrotera
A. chinensis
A. uniflora
A: A. macrotera
B: A. forrestii
(C)
1.00
0.80
0.60
0.40
0.20
0.00
A. macrotera
A. uniflora
A. forrestii
A. chinensis
A. × grandiflora

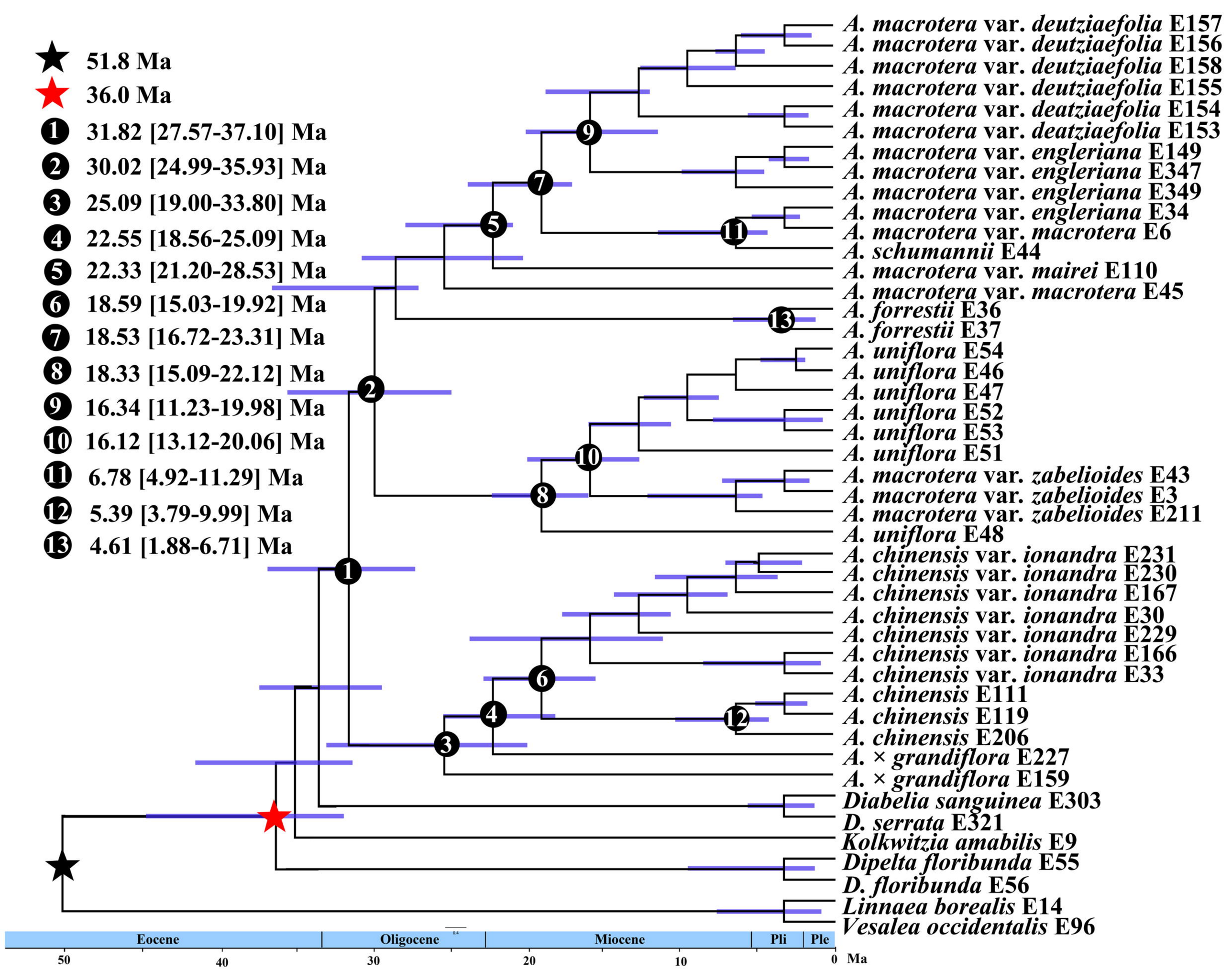
51.8 Ma
36.0 Ma
1 31.82 [27.57-37.10] Ma
2 30.02 [24.99-35.93] Ma
3 25.09 [19.00-33.80] Ma
4 22.55 [18.56-25.09] Ma
5 22.33 [21.20-28.53] Ma
6 18.59 [15.03-19.92] Ma
7 18.53 [16.72-23.31] Ma
8 18.33 [15.09-22.12] Ma
9 16.34 [11.23-19.98] Ma
10 16.12 [13.12-20.06] Ma
11 6.78 [4.92-11.29] Ma
12 5.39 [3.79-9.99] Ma
13 4.61 [1.88-6.71] Ma
A. macrotera var. deutziaefolia E157
A. macrotera var. deutziaefolia E156
A. macrotera var. deutziaefolia E158
A. macrotera var. deutziaefolia E155
A. macrotera var. deatziaefolia E154
A. macrotera var. deatziaefolia E153
A. macrotera var. engleriana E149
A. macrotera var. engleriana E347
A. macrotera var. engleriana E349
A. macrotera var. engleriana E34
A. macrotera var. macrotera E6
A. schumannii E44
A. macrotera var. mairei E110
A. macrotera var. macrotera E45
A. forrestii E36
A. forrestii E37
A. uniflora E54
A. uniflora E46
A. uniflora E47
A. uniflora E52
A. uniflora E53
A. uniflora E51
A. macrotera var. zabelioides E43
A. macrotera var. zabelioides E3
A. macrotera var. zabelioides E211
A. uniflora E48
A. chinensis var. ionandra E231
A. chinensis var. ionandra E230
A. chinensis var. ionandra E167
A. chinensis var. ionandra E30
A. chinensis var. ionandra E229
A. chinensis var. ionandra E166
A. chinensis var. ionandra E33
A. chinensis E111
A. chinensis E119
A. chinensis E206
A. × grandiflora E227
A. × grandiflora E159
Diabelia sanguinea E303
D. serrata E321
Kolkwitzia amabilis E9
Dipelta floribunda E55
D. floribunda E56
Linnaea borealis E14
Vesalea occidentalis E96
Eocene
Oligocene
Miocene
Pli
Ple
50
40
30
20
10
0 Ma

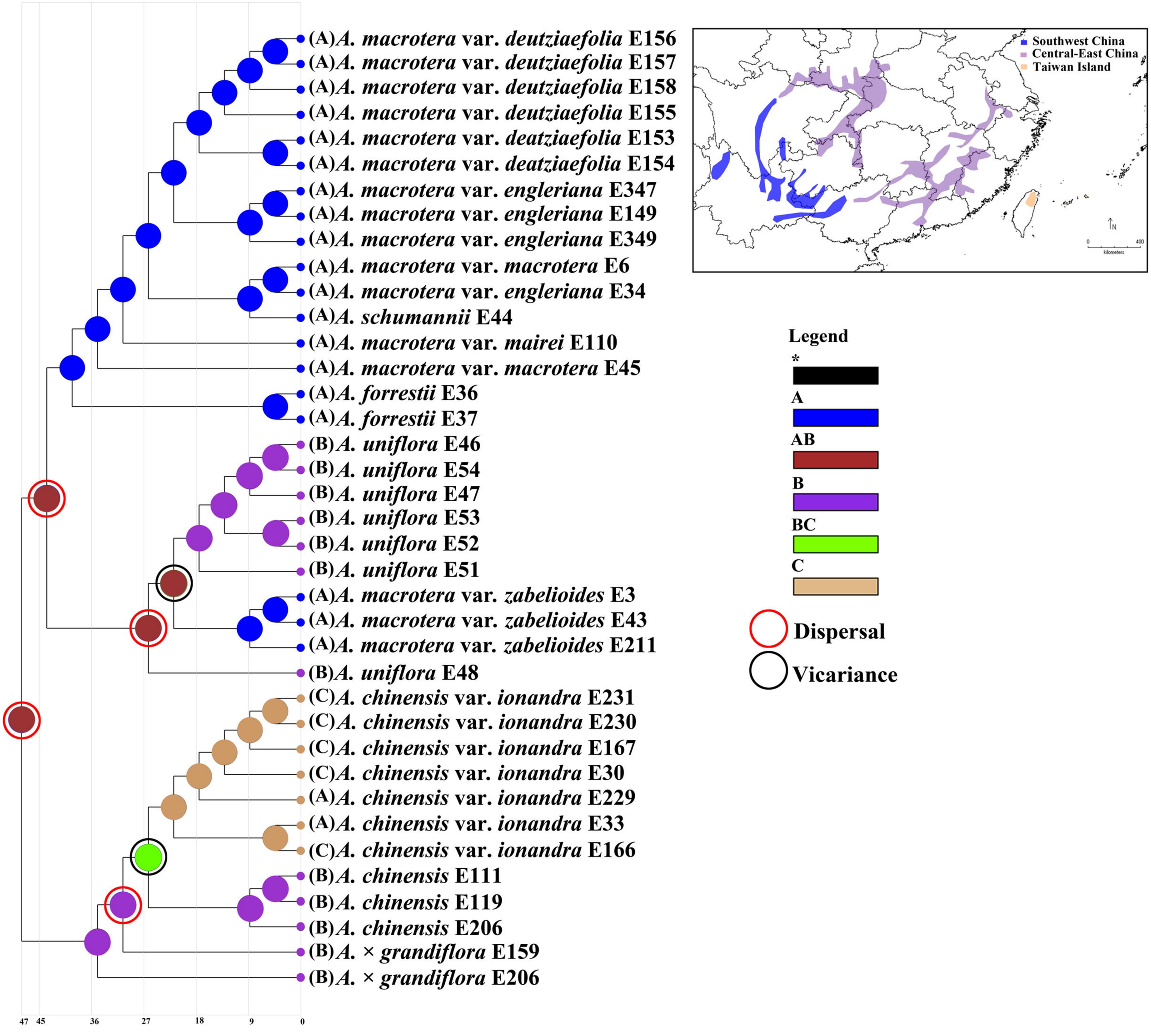
(A)A. macrotera var. deutziaefolia E156
(A)A. macrotera var. deutziaefolia E157
(A)A. macrotera var. deutziaefolia E158
(A)A. macrotera var. deutziaefolia E155
(A)A. macrotera var. deatziaefolia E153
(A)A. macrotera var. deatziaefolia E154
(A)A. macrotera var. engleriana E347
(A)A. macrotera var. engleriana E149
(A)A. macrotera var. engleriana E349
(A)A. macrotera var. macrotera E6
(A)A. macrotera var. engleriana E34
(A)A. schumannii E44
(A)A. macrotera var. mairei E110
(A)A. macrotera var. macrotera E45
(A)A. forrestii E36
(A)A. forrestii E37
(B)A. uniflora E46
(B)A. uniflora E54
(B)A. uniflora E47
(B)A. uniflora E53
(B)A. uniflora E52
(B)A. uniflora E51
(A)A. macrotera var. zabelioides E3
(A)A. macrotera var. zabelioides E43
(A)A. macrotera var. zabelioides E211
(B)A. uniflora E48
(C)A. chinensis var. ionandra E231
(C)A. chinensis var. ionandra E230
(C)A. chinensis var. ionandra E167
(C)A. chinensis var. ionandra E30
(A)A. chinensis var. ionandra E229
(A)A. chinensis var. ionandra E33
(C)A. chinensis var. ionandra E166
(B)A. chinensis E111
(B)A. chinensis E119
(B)A. chinensis E206
(B)A. × grandiflora E159
(B)A. × grandiflora E206
47 45 36 27 18 9 0
Southwest China
Central-East China
Taiwan Island
N
0 400
kilometers
Legend
*
A
AB
B
BC
C
Dispersal
Vicariance

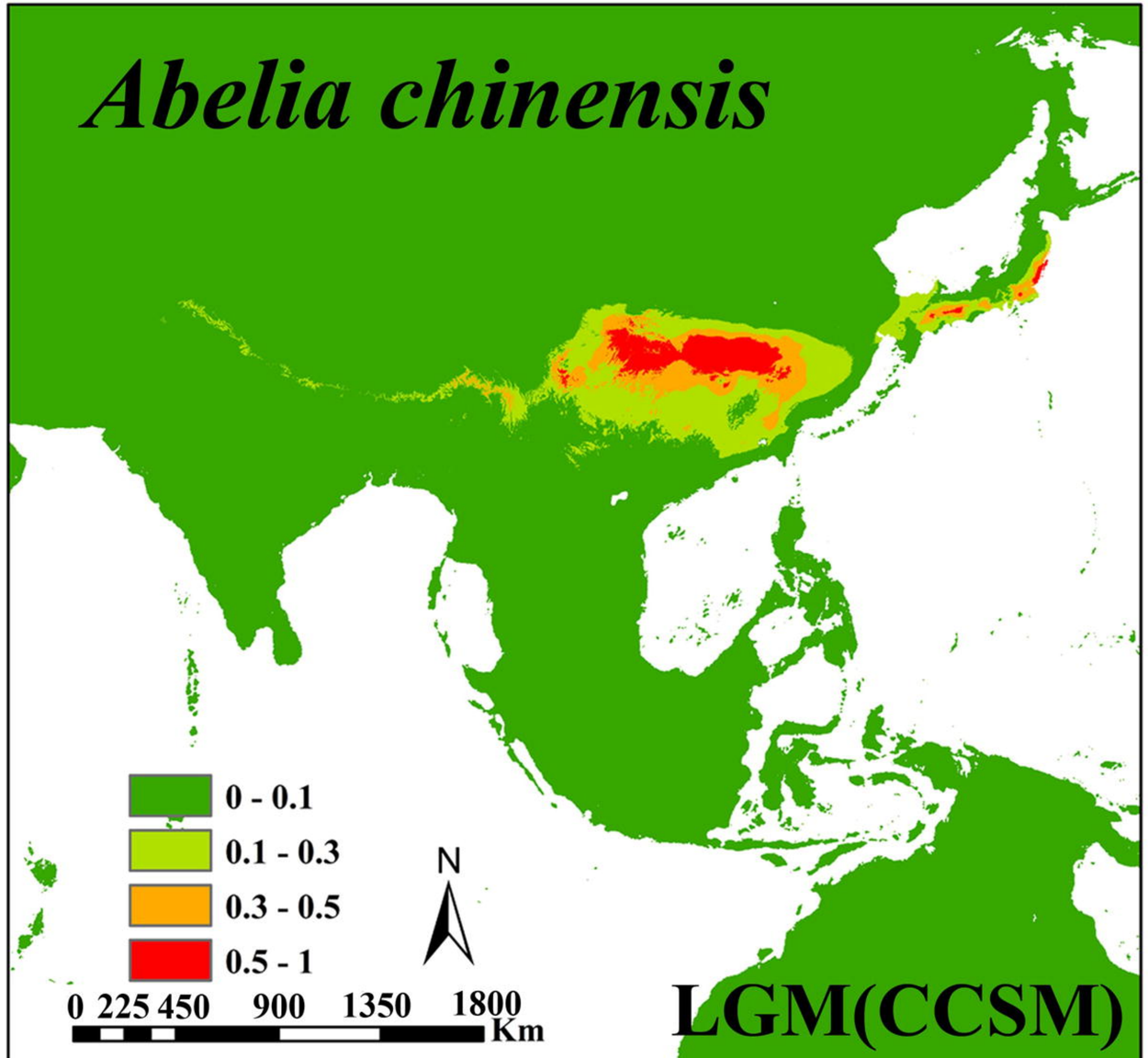
Abelia chinensis
0 - 0.1
0.1 - 0.3
0.3 - 0.5
0.5 - 1
N
0 225 450 900 1350 1800
Km
LGM(CCSM)

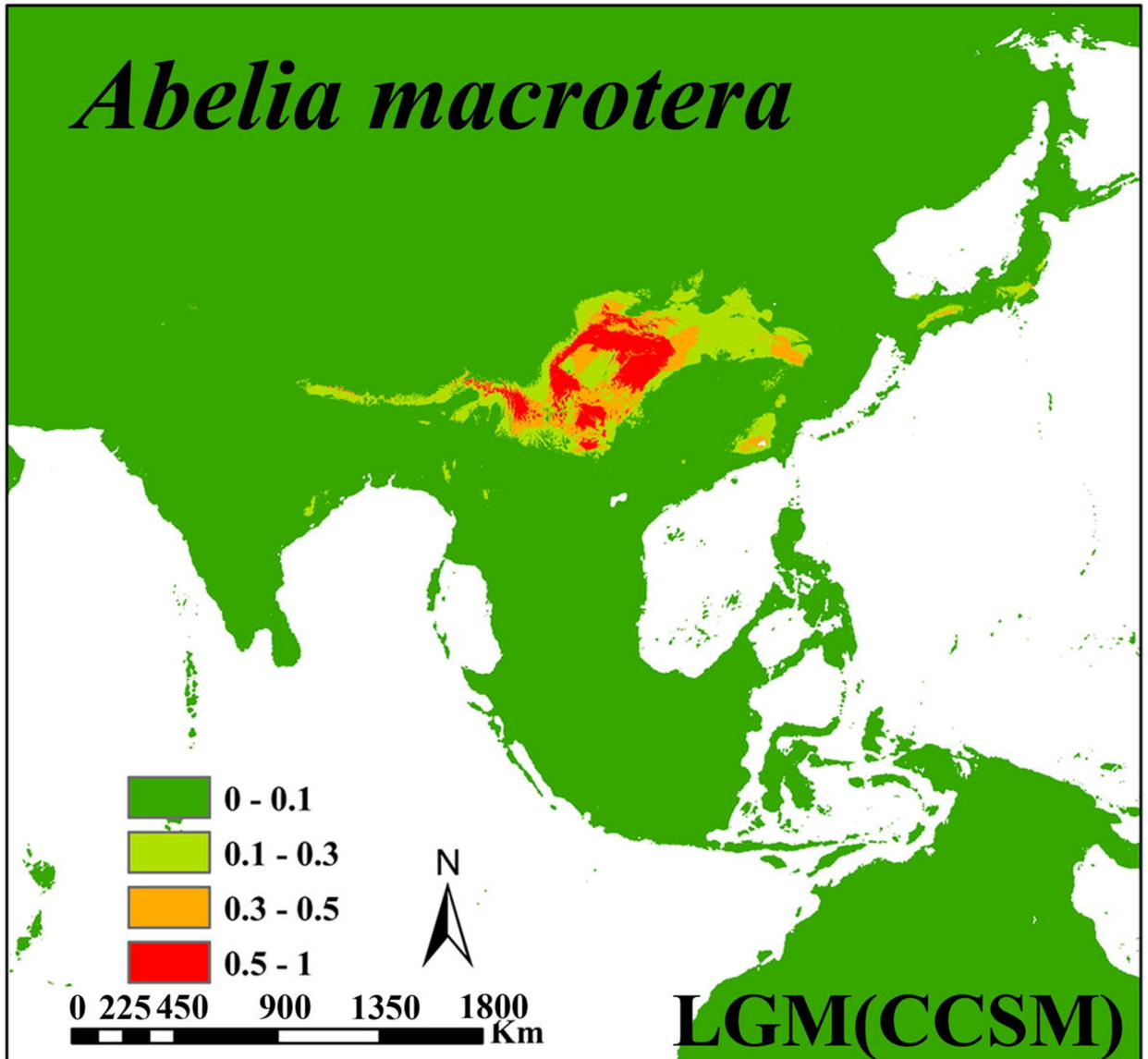
Abelia macrotera
0 - 0.1
0.1 - 0.3
0.3 - 0.5
0.5 - 1
N
0 225 450 900 1350 1800
Km
LGM(CCSM)

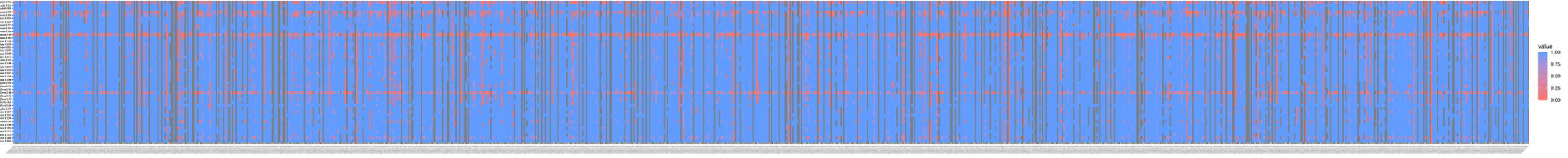
value
1.00
0.75
0.50
0.25
0.00

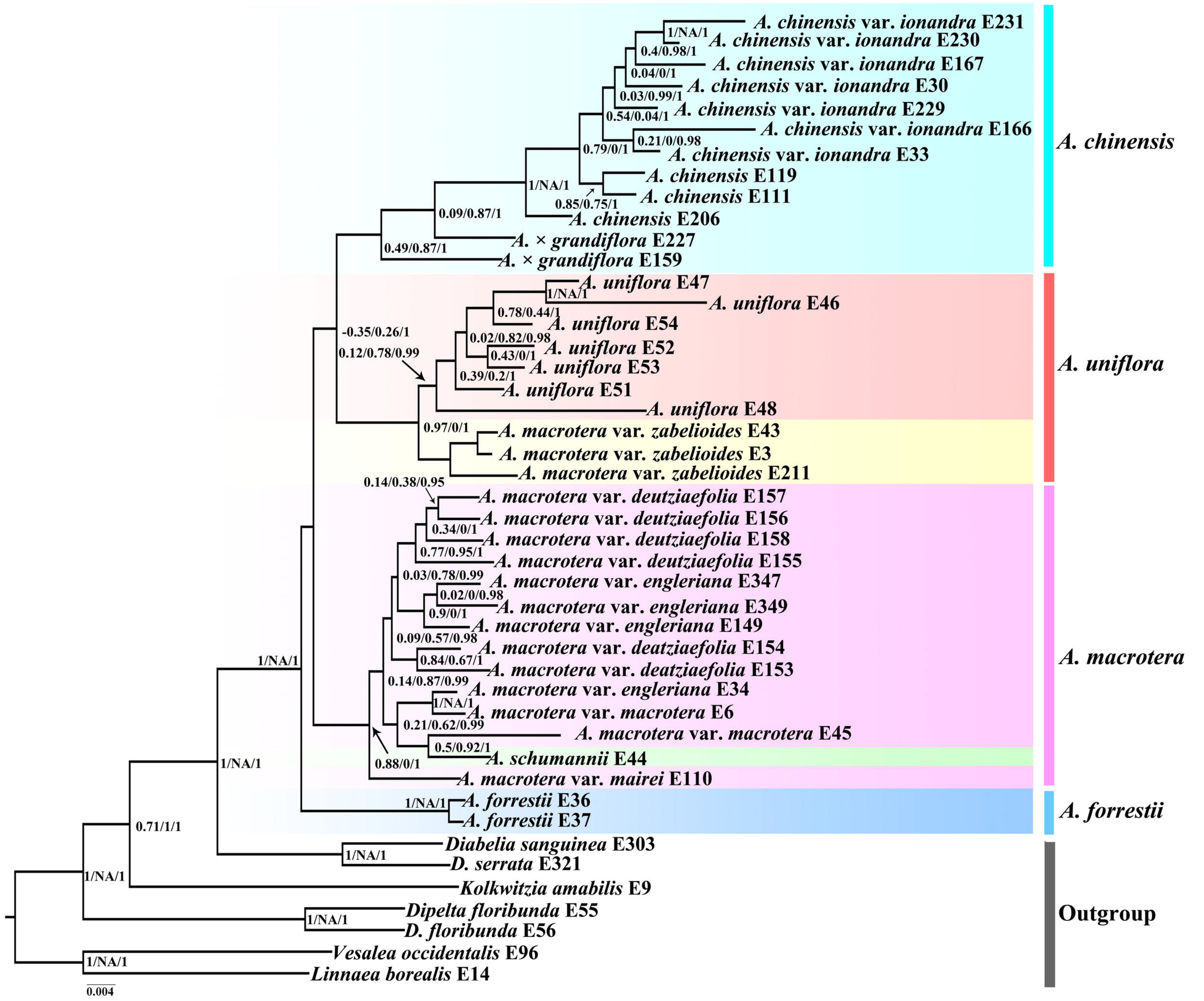
A. chinensis var. ionandra E231
A. chinensis var. ionandra E230
A. chinensis var. ionandra E167
A. chinensis var. ionandra E30
A. chinensis var. ionandra E229
A. chinensis var. ionandra E166
A. chinensis var. ionandra E33
A. chinensis E119
A. chinensis E111
A. chinensis E206
A. × grandiflora E227
A. × grandiflora E159
A. uniflora E47
A. uniflora E46
A. uniflora E54
A. uniflora E52
A. uniflora E53
A. uniflora E51
A. uniflora E48
A. macrotera var. zabelioides E43
A. macrotera var. zabelioides E3
A. macrotera var. zabelioides E211
A. macrotera var. deutziaefolia E157
A. macrotera var. deutziaefolia E156
A. macrotera var. deutziaefolia E158
A. macrotera var. deutziaefolia E155
A. macrotera var. engleriana E347
A. macrotera var. engleriana E349
A. macrotera var. engleriana E149
A. macrotera var. deatziaefolia E154
A. macrotera var. deatziaefolia E153
A. macrotera var. engleriana E34
A. macrotera var. macrotera E6
A. macrotera var. macrotera E45
A. schumannii E44
A. macrotera var. mairei E110
A. forrestii E36
A. forrestii E37
Diabelia sanguinea E303
D. serrata E321
Kolkwitzia amabilis E9
Dipelta floribunda E55
D. floribunda E56
Vesalea occidentalis E96
Linnaea borealis E14
A. chinensis
A. uniflora
A. macrotera
A. forrestii
Outgroup
1/NA/1
0.4/0.98/1
0.04/0/1
0.03/0.99/1
0.54/0.04/1
0.21/0/0.98
0.79/0/1
1/NA/1
0.85/0.75/1
0.09/0.87/1
0.49/0.87/1
1/NA/1
0.78/0.44/1
-0.35/0.26/1
0.12/0.78/0.99
0.02/0.82/0.98
0.43/0/1
0.39/0.2/1
0.97/0/1
0.14/0.38/0.95
0.34/0/1
0.77/0.95/1
0.03/0.78/0.99
0.02/0/0.98
0.9/0/1
0.09/0.57/0.98
0.84/0.67/1
1/NA/1
0.14/0.87/0.99
1/NA/1
0.21/0.62/0.99
0.5/0.92/1
0.88/0/1
1/NA/1
1/NA/1
0.71/1/1
1/NA/1
1/NA/1
1/NA/1
1/NA/1
0.004

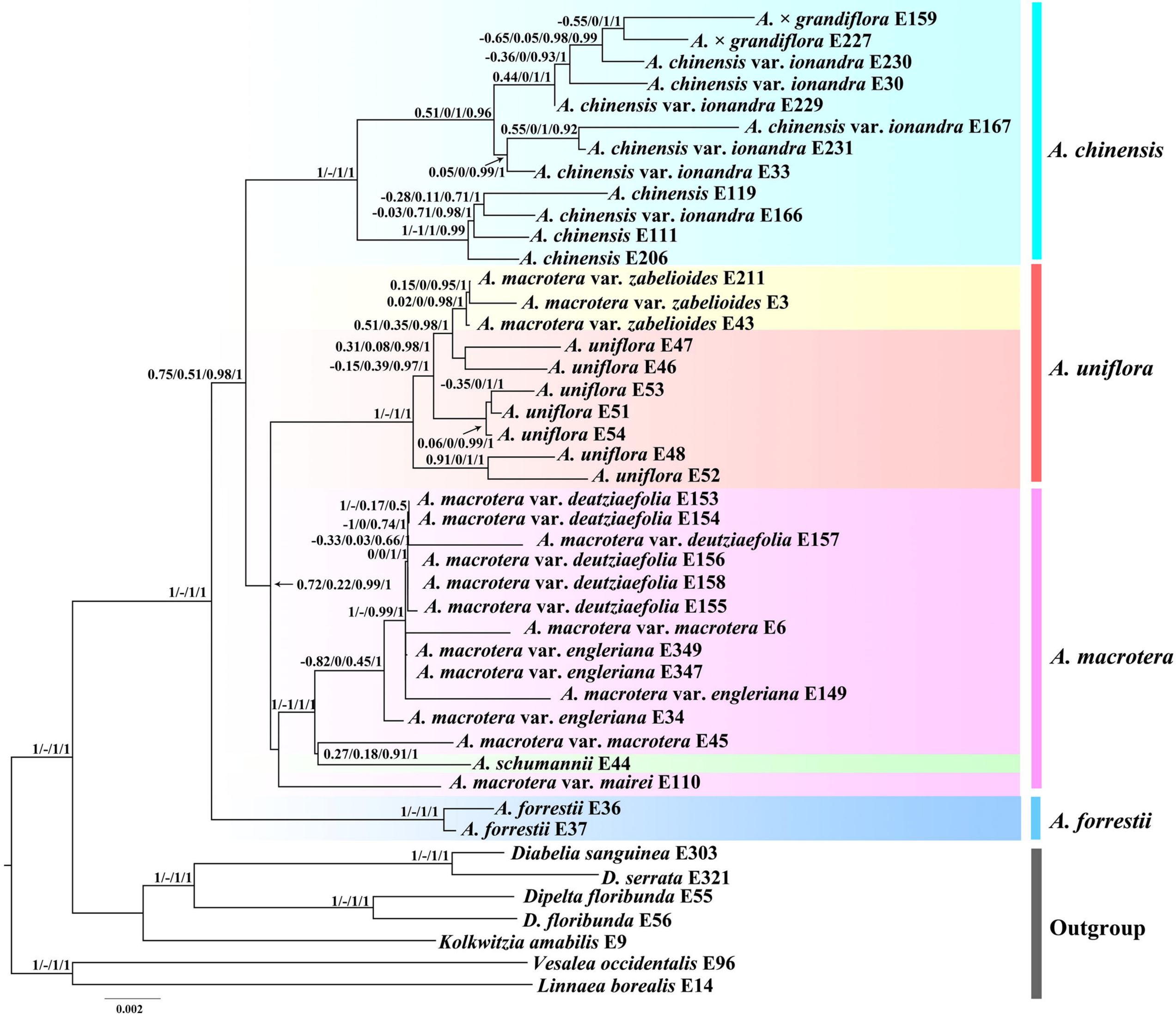
A. × grandiflora E159
A. × grandiflora E227
A. chinensis var. ionandra E230
A. chinensis var. ionandra E30
A. chinensis var. ionandra E229
A. chinensis var. ionandra E167
A. chinensis var. ionandra E231
A. chinensis var. ionandra E33
A. chinensis E119
A. chinensis var. ionandra E166
A. chinensis E111
A. chinensis E206
A. macrotera var. zabelioides E211
A. macrotera var. zabelioides E3
A. macrotera var. zabelioides E43
A. uniflora E47
A. uniflora E46
A. uniflora E53
A. uniflora E51
A. uniflora E54
A. uniflora E48
A. uniflora E52
A. macrotera var. deatziaefolia E153
A. macrotera var. deatziaefolia E154
A. macrotera var. deutziaefolia E157
A. macrotera var. deutziaefolia E156
A. macrotera var. deutziaefolia E158
A. macrotera var. deutziaefolia E155
A. macrotera var. macrotera E6
A. macrotera var. engleriana E349
A. macrotera var. engleriana E347
A. macrotera var. engleriana E149
A. macrotera var. engleriana E34
A. macrotera var. macrotera E45
A. schumannii E44
A. macrotera var. mairei E110
A. forrestii E36
A. forrestii E37
Diabelia sanguinea E303
D. serrata E321
Dipelta floribunda E55
D. floribunda E56
Kolkwitzia amabilis E9
Vesalea occidentalis E96
Linnaea borealis E14
A. chinensis
A. uniflora
A. macrotera
A. forrestii
Outgroup
0.002

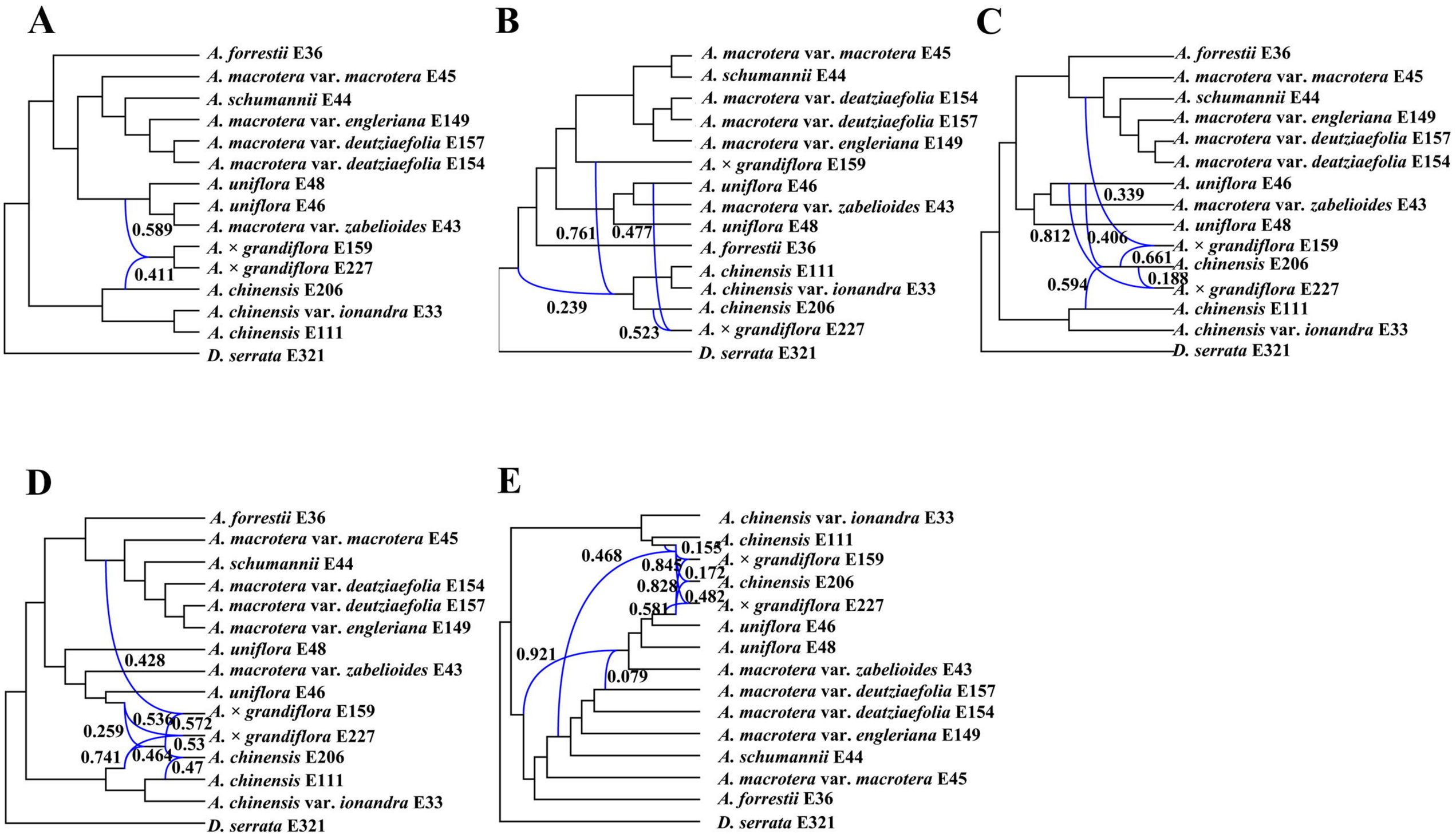
A
A. forrestii E36
A. macrotera var. macrotera E45
A. schumannii E44
A. macrotera var. engleriana E149
A. macrotera var. deutziaefolia E157
A. macrotera var. deatziaefolia E154
A. uniflora E48
A. uniflora E46
A. macrotera var. zabelioides E43
A. × grandiflora E159
A. × grandiflora E227
A. chinensis E206
A. chinensis var. ionandra E33
A. chinensis E111
D. serrata E321
0.589
0.411
B
A. macrotera var. macrotera E45
A. schumannii E44
A. macrotera var. deatziaefolia E154
A. macrotera var. deutziaefolia E157
A. macrotera var. engleriana E149
A. × grandiflora E159
A. uniflora E46
A. macrotera var. zabelioides E43
A. uniflora E48
A. forrestii E36
A. chinensis E111
A. chinensis var. ionandra E33
A. chinensis E206
A. × grandiflora E227
D. serrata E321
0.761
0.477
0.239
0.523
C
A. forrestii E36
A. macrotera var. macrotera E45
A. schumannii E44
A. macrotera var. engleriana E149
A. macrotera var. deutziaefolia E157
A. macrotera var. deatziaefolia E154
A. uniflora E46
A. macrotera var. zabelioides E43
A. uniflora E48
A. × grandiflora E159
A. chinensis E206
A. × grandiflora E227
A. chinensis E111
A. chinensis var. ionandra E33
D. serrata E321
0.339
0.812
0.406
0.661
0.188
0.594
D
A. forrestii E36
A. macrotera var. macrotera E45
A. schumannii E44
A. macrotera var. deatziaefolia E154
A. macrotera var. deutziaefolia E157
A. macrotera var. engleriana E149
A. uniflora E48
A. macrotera var. zabelioides E43
A. uniflora E46
A. × grandiflora E159
A. × grandiflora E227
A. chinensis E206
A. chinensis E111
A. chinensis var. ionandra E33
D. serrata E321
0.428
0.259
0.741
0.536
0.572
0.53
0.464
0.47
E
A. chinensis var. ionandra E33
A. chinensis E111
A. × grandiflora E159
A. chinensis E206
A. × grandiflora E227
A. uniflora E46
A. uniflora E48
A. macrotera var. zabelioides E43
A. macrotera var. deutziaefolia E157
A. macrotera var. deatziaefolia E154
A. macrotera var. engleriana E149
A. schumannii E44
A. macrotera var. macrotera E45
A. forrestii E36
D. serrata E321
0.468
0.155
0.845
0.172
0.828
0.482
0.581
0.921
0.079

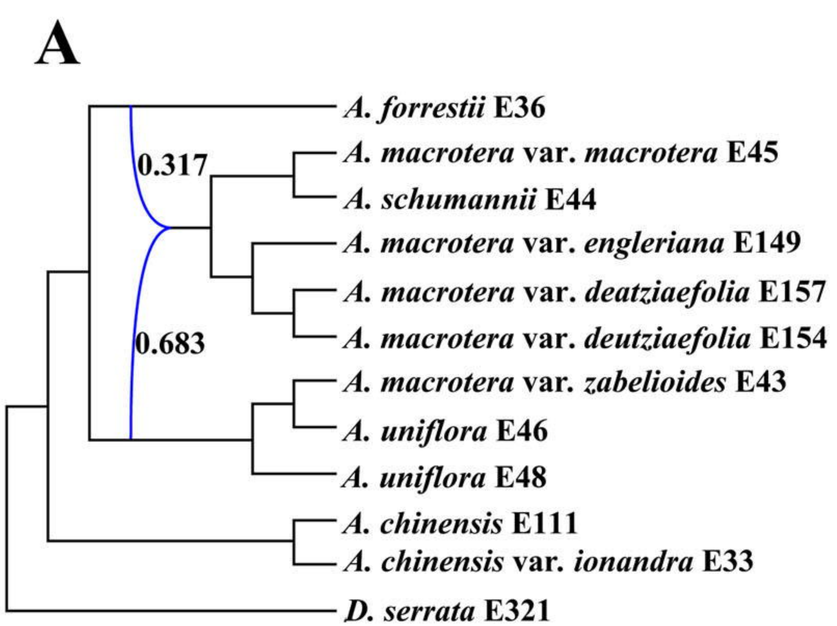
A
A. forrestii E36
A. macrotera var. macrotera E45
A. schumannii E44
A. macrotera var. engleriana E149
A. macrotera var. deatziaefolia E157
A. macrotera var. deutziaefolia E154
A. macrotera var. zabelioides E43
A. uniflora E46
A. uniflora E48
A. chinensis E111
A. chinensis var. ionandra E33
D. serrata E321
0.317
0.683

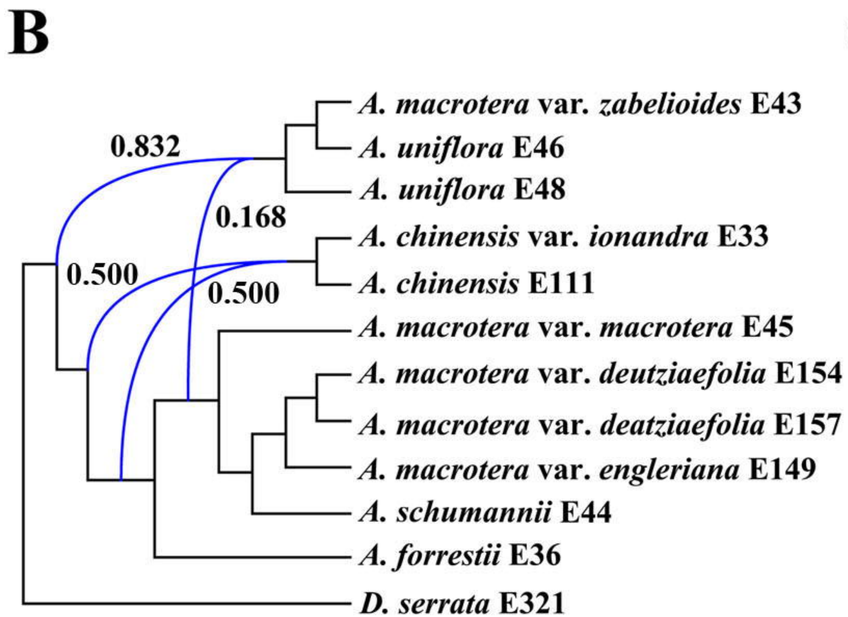
B
A. macrotera var. zabelioides E43
A. uniflora E46
A. uniflora E48
A. chinensis var. ionandra E33
A. chinensis E111
A. macrotera var. macrotera E45
A. macrotera var. deutziaefolia E154
A. macrotera var. deatziaefolia E157
A. macrotera var. engleriana E149
A. schumannii E44
A. forrestii E36
D. serrata E321
0.832
0.168
0.500
0.500

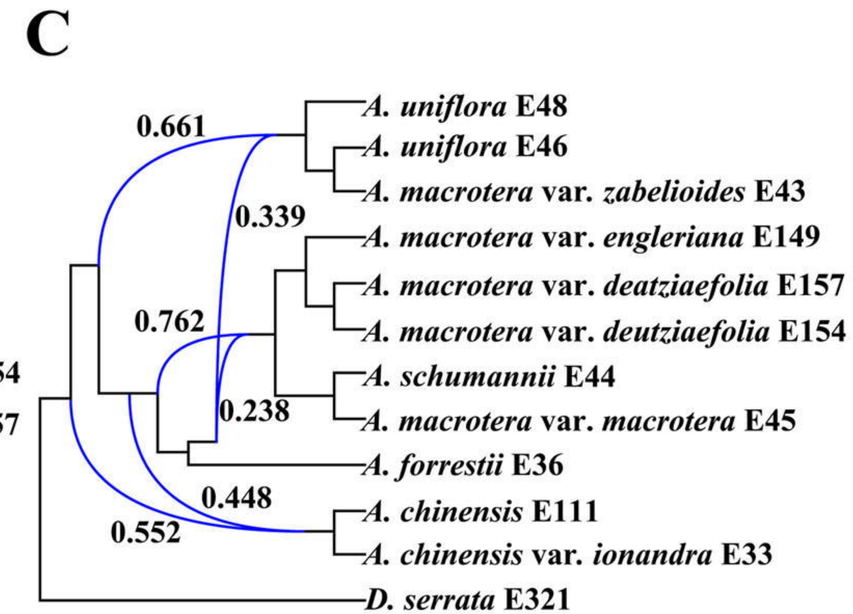
C
A. uniflora E48
A. uniflora E46
A. macrotera var. zabelioides E43
A. macrotera var. engleriana E149
A. macrotera var. deatziaefolia E157
A. macrotera var. deutziaefolia E154
A. schumannii E44
A. macrotera var. macrotera E45
A. forrestii E36
A. chinensis E111
A. chinensis var. ionandra E33
D. serrata E321
0.661
0.339
0.762
0.238
0.448
0.552

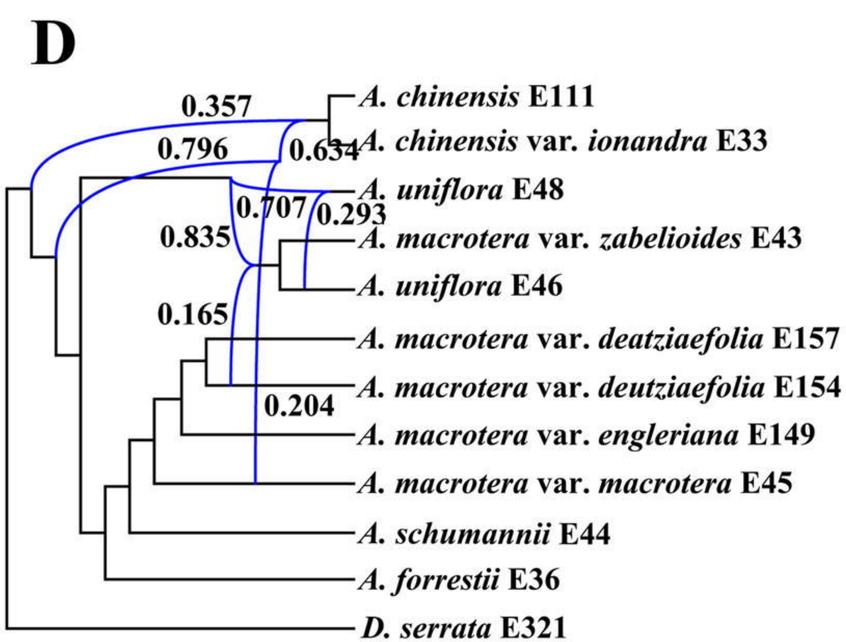
D
A. chinensis E111
A. chinensis var. ionandra E33
A. uniflora E48
A. macrotera var. zabelioides E43
A. uniflora E46
A. macrotera var. deatziaefolia E157
A. macrotera var. deutziaefolia E154
A. macrotera var. engleriana E149
A. macrotera var. macrotera E45
A. schumannii E44
A. forrestii E36
D. serrata E321
0.357
0.796
0.634
0.707
0.293
0.835
0.165
0.204

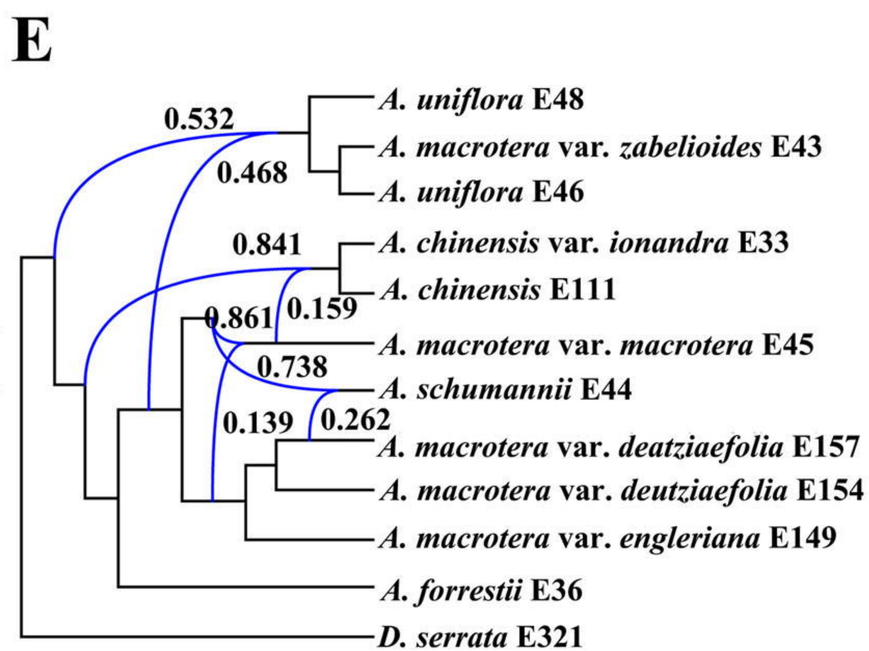
E
A. uniflora E48
A. macrotera var. zabelioides E43
A. uniflora E46
A. chinensis var. ionandra E33
A. chinensis E111
A. macrotera var. macrotera E45
A. schumannii E44
A. macrotera var. deatziaefolia E157
A. macrotera var. deutziaefolia E154
A. macrotera var. engleriana E149
A. forrestii E36
D. serrata E321
0.532
0.468
0.841
0.861
0.159
0.738
0.139
0.262

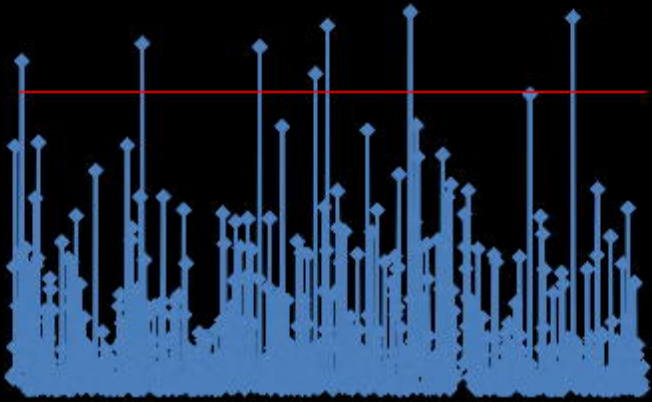

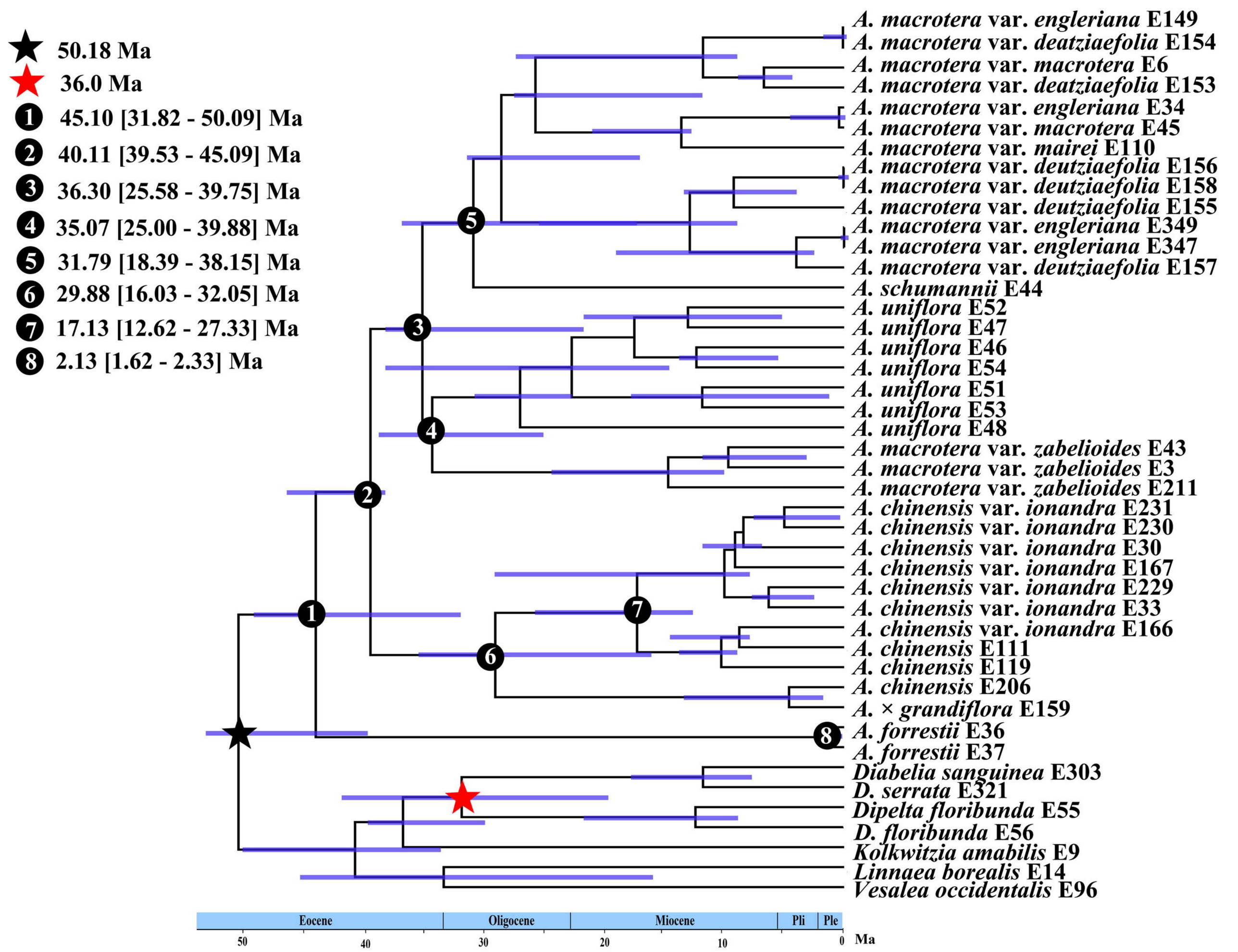
50.18 Ma
36.0 Ma
1 45.10 [31.82 - 50.09] Ma
2 40.11 [39.53 - 45.09] Ma
3 36.30 [25.58 - 39.75] Ma
4 35.07 [25.00 - 39.88] Ma
5 31.79 [18.39 - 38.15] Ma
6 29.88 [16.03 - 32.05] Ma
7 17.13 [12.62 - 27.33] Ma
8 2.13 [1.62 - 2.33] Ma
A. macrotera var. engleriana E149
A. macrotera var. deatziaefolia E154
A. macrotera var. macrotera E6
A. macrotera var. deatziaefolia E153
A. macrotera var. engleriana E34
A. macrotera var. macrotera E45
A. macrotera var. mairei E110
A. macrotera var. deutziaefolia E156
A. macrotera var. deutziaefolia E158
A. macrotera var. deutziaefolia E155
A. macrotera var. engleriana E349
A. macrotera var. engleriana E347
A. macrotera var. deutziaefolia E157
A. schumannii E44
A. uniflora E52
A. uniflora E47
A. uniflora E46
A. uniflora E54
A. uniflora E51
A. uniflora E53
A. uniflora E48
A. macrotera var. zabelioides E43
A. macrotera var. zabelioides E3
A. macrotera var. zabelioides E211
A. chinensis var. ionandra E231
A. chinensis var. ionandra E230
A. chinensis var. ionandra E30
A. chinensis var. ionandra E167
A. chinensis var. ionandra E229
A. chinensis var. ionandra E33
A. chinensis var. ionandra E166
A. chinensis E111
A. chinensis E119
A. chinensis E206
A. × grandiflora E159
A. forrestii E36
A. forrestii E37
Diabelia sanguinea E303
D. serrata E321
Dipelta floribunda E55
D. floribunda E56
Kolkwitzia amabilis E9
Linnaea borealis E14
Vesalea occidentalis E96
Eocene
Oligocene
Miocene
Pli
Ple
50
40
30
20
10
0
Ma

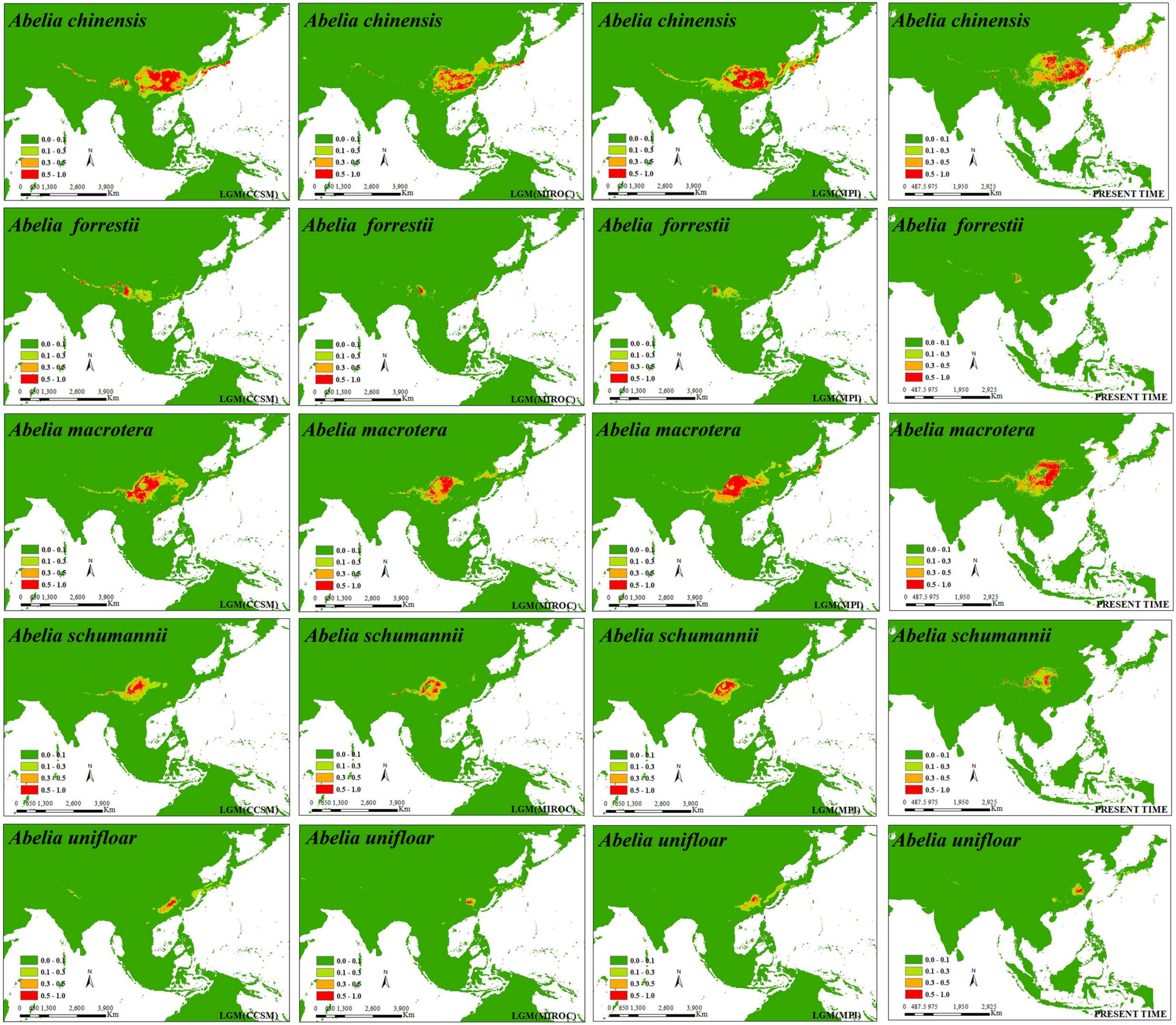
Abelia chinensis
LGM(CCSM)
Abelia chinensis
LGM(MIROC)
Abelia chinensis
LGM(MPI)
Abelia chinensis
PRESENT TIME
Abelia forrestii
LGM(CCSM)
Abelia forrestii
LGM(MIROC)
Abelia forrestii
LGM(MPI)
Abelia forrestii
PRESENT TIME
Abelia macrotera
LGM(CCSM)
Abelia macrotera
LGM(MIROC)
Abelia macrotera
LGM(MPI)
Abelia macrotera
PRESENT TIME
Abelia schumannii
LGM(CCSM)
Abelia schumannii
LGM(MIROC)
Abelia schumannii
LGM(MPI)
Abelia schumannii
PRESENT TIME
Abelia unifloar
LGM(CCSM)
Abelia unifloar
LGM(MIROC)
Abelia unifloar
LGM(MPI)
Abelia unifloar
PRESENT TIME
0.0 - 0.1
0.1 - 0.3
0.3 - 0.5
0.5 - 1.0
N
0 650 1,300 2,600 3,900 Km
0 487.5 975 1,950 2,925 Km